Open Mathematics

Research Article

Jing-Gai Li and Chun-Gang Zhu*

Curve and surface construction based on the generalized toric-Bernstein basis functions

https://doi.org/10.1515/math-2020-0004
Received June 28, 2019; accepted January 18, 2020

Abstract: The construction of parametric curve and surface plays an important role in computer aided geometric design (CAGD), computer aided design (CAD), and geometric modeling. In this paper, we define a new kind of blending functions associated with a real points set, called generalized toric-Bernstein (GT-Bernstein) basis functions. Then, the generalized toric-Bézier (GT-Bézier) curves and surfaces are constructed based on the GT-Bernstein basis functions, which are the projections of the (irrational) toric varieties in fact and the generalizations of the classical rational Bézier curves/surfaces and toric surface patches. Furthermore, we also study the properties of the presented curves and surfaces, including the limiting properties of weights and knots. Some representative examples verify the properties and results.

Keywords: Bernstein basis functions, basis functions, Bézier curves and surfaces, curve and surface design, toric surface patches

MSC 2010: 65D17, 68U07

1 Introduction

In Computer Aided Geometric Design (CAGD) and Computed Aided Design (CAD), Bézier curves/surfaces play the central role [1, 2]. They were firstly described by French engineer Pierre Bézier to design automobile bodies in 1962 [3]. From the viewpoint of algebraic geometry, Bézier curves/surfaces are projections of real toric varieties from higher-dimensional space. In 1992, Probably Warren [4] was the first who noticed that the real toric variety can be applied in CAGD. In 2002, Krasauskas [5] proposed a kind of rational multisided surface, namely toric surface, which is conncened with a finite set of integer lattice points based on the toric ideals and toric varieties. The toric surface is degenerated into rational Bézier curve if the lattice points set is constrained to a one-dimensional integer points. What's more, the tensor product Bézier surfaces and Bézier triangles are also special cases of the toric surface. García-Puente et al. [6] indicated that limiting surface of toric patch is the regular control surface when all weights tend to infinity, which is called the toric degeneration. Since toric surface patches are a muliti-sided generalization of Bézier surfaces, compared with the Bézier scheme, they require fewer surface patches in applications such as data fitting, blending surfaces, hole-filling and so on, and the overall smoothness is better.

In recent years, the parametric curves/surfaces construction based on different basis functions have been studied by many scholars. Zhang [7, 8] investigated curves in the space $span\{1, t, \cos t, \sin t\}$. Chen and Wang et al. [9, 10] defined the C-Bézier curve and the C-B spline curve (NUAT B-spline curve) by extending the space of mixed algebra and trigonometric polynomial. Oruç and Phillips [11] defined the q-Bézier curve

Jing-Gai Li: School of Mathematical Sciences, Dalian University of Technology, China; E-mail: Lijinggaim@mail.dlut.edu.cn
***Corresponding Author: Chun-Gang Zhu:** School of Mathematical Sciences, Dalian University of Technology, China; E-mail: cgzhu@dlut.edu.cn

based on the q-Bernstein operator which was constructed by Phillips [12]. Han et al. [13] presented the generalizations of Bézier curves and the tensor product surfaces. These curves and surfaces are based on the Lupaş q-analogue of Bernstein operator. Cai et al. [14] presented a new generalization of λ-Bernstein operators based on q-integers and established a statistical approximation theorem. Hu et al. [15] presented a novel shape-adjustable generalized Bézier curve with multiple shape parameters and discussed its applications to surface modeling in engineering. Hu and Wu [16] presented a kind of generalized quartic H-Bézier basis functions with four shape parameters. And the expression and some properties of the corresponding curves were discussed. Schaback [17] gave an introduction to certain techniques for the construction of surfaces from scattered data, which emphasis is putting on interpolation methods using compactly supported radial basis functions. Goldman and Simeonov [18] studied the properties of quantum Bernstein bases and quantum Bézier curves by introducing a new variant of the blossom. Zhou and Cai [19] constructed a triangular Meyer-König-Zeller surface based on bivariate Meyer-König-Zeller operator. Zhou et al. [20] constructed two kinds of bivariate $S-\lambda$ basis functions, tensor product and triangular $S-\lambda$ basis functions by means of the technique of generating functions and transformation factors. Moreover, the corresponding two kinds of $S-\lambda$ surfaces were studied. Salvi and Várady [21] described a new patch that extends the concept of generalized Bézier patches [22] to concave polygonal domains.

Most of the basis functions constructing curves and surfaces defined above are represented in non-negative integer power forms. At present, some researchers have put many efforts on the construction of curves and surfaces based on basis functions with rational or irrational number powers . The multiquadric (MQ) function is a radial basis function (RBF) with the rational number power form, which is widely used in numerical analysis and scientific computing [17]. In 2015, Zhu et al. [23] extended the Bernstein basis functions and then constructed $\alpha\beta$-Bernstein-like basis with two exponential shape parameters α and β with real number degrees.

García-Puente and Sottile [24] showed that tuning a pentagonal toric patch by lattice points $\widetilde{\mathcal{A}}$ (see Figure 1(b)) instead of $\mathcal{A}$ (see Figure 1(a)) to achieve linear precision, where $\widetilde{\mathcal{A}}$ contains three non-integer points. In 2008, Craciun et al. [25] studied the theory of toric varieties defined by generally real lattice sets, which were applied in algebraic statistics known as toric model [26] and studied the geometric properties of toric surfaces. In 2015, Postinghel et al. [27] presented the degenerations of real irrational toric varieties defined by generally real number set. Pir and Sottile studied the theory of irrational toric varieties in [28]. Li et al. preliminarily studied the T-Bézier curve constructed by the real points in [29].

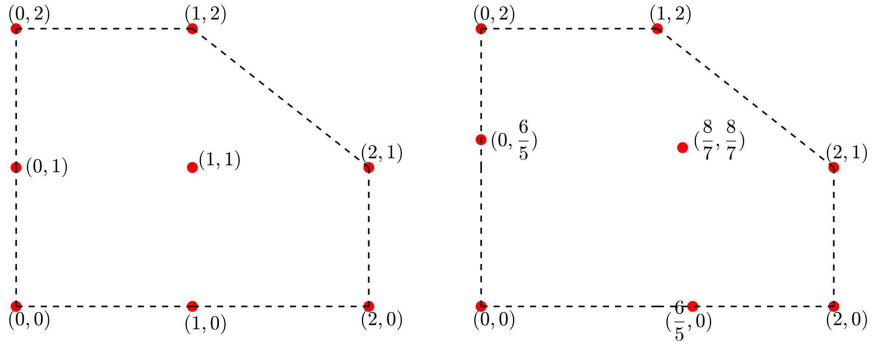

(a) Lattice points $\mathcal{A}$ (b) Lattice points $\widetilde{\mathcal{A}}$

Figure 1: Lattice points $\mathcal{A}$ and $\widetilde{\mathcal{A}}$.

In this paper, inspired by above methods, we define a new kind of blending functions associated with a real points set, called generalized toric-Bernstein (GT-Bernstein) basis functions. The degree of GT-Bernstein basis functions is an arbitrary real number. Then, the corresponding generalized toric-Bézier (GT-Bézier) curves and surfaces are constructed, which are the projections of the (irrational) toric varieties in fact and

the generalizations of the classical rational Bézier curves/surfaces and toric surface patches. Furthermore, we also study the properties of the presented curves and surfaces, including the limiting properties of weights and knots. We generalize the lattice points in the definition of toric surface patches to the real points in this paper, and this leads to construct a wider range of shapes for applications. We may construct GT-Bézier surfaces with linear precision for barycentric coordinate construction (as Figure 1 shows), we can apply the limiting properties of weights for shape deformation, computer animation and costume designing as [30] did, and we also can construct multisided surface patch from a given points by progressive iteration approximation (PIA) by method in [31].

The rest of this paper is organized as follows. In Section 2, the generalized toric-Bernstein basis functions are defined and the properties of the basis are studied. And then a class of generalized Bézier curve is constructed in Section 3, which is the generalization of the classical rational Bézier curve. In Section 4, we construct a new kind of multisided parametric surface by bivariate generalized toric-Bernstein basis functions. At last, we conclude the whole paper and point out the future work in Section 5.

2 Generalized toric-Bernstein basis functions

It is well known that toric Bernstein basis functions depend on the finite set of integer lattice points $\mathcal{A}$ and boundary functions of the convex hull(lattice polygon) $\Delta_{\mathcal{A}}$ of $\mathcal{A}$. When the lattice polygon $\Delta_{\mathcal{A}}$ is a standard triangle or a rectangle, if we take appropriate coefficients, the toric Bernstein basis functions degenerate into the classical Bernstein basis functions after the parameter transformation. So they are the generalizations of the classical Bernstein basis functions. In this section, we generalize the toric Bernstein basis functions to finite set of real points, and give the definitions of generalized toric-Bernstein basis functions in one and two dimensions.

2.1 Univariate generalized toric-Bernstein basis functions

Consider $\mathcal{A} = \{a_0, a_1, \cdots, a_n\} \subset \mathbb{R}$ with $a_0 \le a_1 \le \cdots \le a_{n-1} \le a_n$, and $\Delta_{\mathcal{A}} = [a_0, a_n]$. Obviously, the endpoints of $\Delta_{\mathcal{A}}$ are points a_0 and a_n and we assume $a_0 < a_n$. Set $h_0(t) = k_0(t - a_0)$ and $h_1(t) = k_1(a_n - t)$, where k_0, k_1 are positive real numbers such that $h_0(t) \ge 0$, $h_1(t) \ge 0$, $t \in \Delta_{\mathcal{A}}$. Then, basis functions indexed by $\mathcal{A}$ can be constructed as follow.

Definition 1. *Let $\mathcal{A} = \{a_0, a_1, \cdots, a_n\} \subset \mathbb{R}$ with $a_0 \le a_1 \le \cdots \le a_{n-1} \le a_n$ and $a_0 < a_n$. Then, for any point a_i in $\mathcal{A}$, we define the generalized toric-Bernstein (GT-Bernstein) basis functions as*

$$\beta_{a_i}(t) = c_{a_i} h_0(t)^{h_0(a_i)} h_1(t)^{h_1(a_i)}, \quad t \in \Delta_{\mathcal{A}}, \tag{1}$$

where coefficient $c_{a_i} > 0$ and a_i is called knot.

The rational form of the GT-Bernstein basis $\beta_{a_i}(t)$ is

$$T_{a_i}(t) = \frac{\omega_{a_i}\beta_{a_i}(t)}{\sum_{i=0}^{n} \omega_{a_i}\beta_{a_i}(t)}, \quad t \in \Delta_{\mathcal{A}}, \tag{2}$$

where $\omega_{a_i} > 0$ is called weight.

Remark 1. *The GT-Bernstein basis $\{\beta_{a_i}(t)\}$ defined by equation (1) depends on the selection of the coefficients k_0 and k_1. Since any positive real numbers can be selected, if there is no special explanation, we set $k_0 = k_1 = 1$. We will show that the curve defined by $\{\beta_{a_i}(t)\}$ is independent of k_0 and k_1 in Section 3.*

Example 1. *Let* $a_0 = 0, a_1 = \frac{\sqrt{2}}{4}, a_2 = \frac{1}{2}, a_3 = \frac{\sqrt{2}}{2}, a_4 = 1$ *and* $c_{a_0} = \frac{1}{2}, c_{a_1} = 1, c_{a_2} = \frac{3}{2}, c_{a_3} = \frac{7}{10}, c_{a_4} = \frac{9}{10}$. *By (1), we have*

$$\beta_{a_0}(t) = \frac{1}{2}(1-t),\ \beta_{a_1}(t) = t^{\frac{\sqrt{2}}{4}}(1-t)^{1-\frac{\sqrt{2}}{4}},$$
$$\beta_{a_2}(t) = \frac{3}{2}t^{\frac{1}{2}}(1-t)^{\frac{1}{2}},\ \beta_{a_3}(t) = \frac{7}{10}t^{\frac{\sqrt{2}}{2}}(1-t)^{1-\frac{\sqrt{2}}{2}},\ \beta_{a_4}(t) = \frac{9}{10}t,$$

and the basis functions $\beta_{a_i}(t)$ *on* $\Delta_{\mathcal{A}} = [0, 1]$ *are shown in Figure 2. The changes of basis function* $\beta_{a_2}(t)$ *while coefficient* c_{a_2} *varying as shown in Figure 3 (the coefficients of curves from bottom to top are* $0.1, 0.7, 1.5, 1.9$ *respectively), which shows that the coefficient mainly affects the function value of the basis function at each point. However, the changes of the basis function* $\beta_{a_2}(t)$ *when its corresponding knot changes are shown in Figure 4 (the knots corresponding to curves from left to right are* $\frac{\sqrt{2}}{5}, \frac{1}{2}, \frac{\sqrt{5}}{3}$ *respectively), which means that the knot mainly affect the positions of the maximum point of the basis function.*

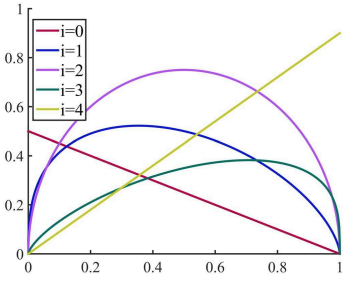

Figure 2: GT-Bernstein basis.

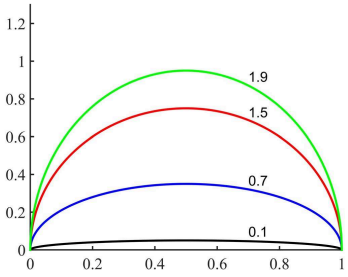

Figure 3: Effect of coefficient changing on GT-Bernstein basis.

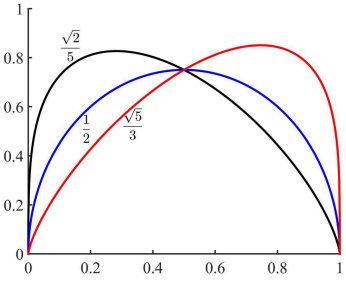

Figure 4: Effect of knot changing on GT-Bernstein basis.

From Definition 1 and rational form (2), some properties of the basis functions $\{T_{a_i}(t)\}$ can be obtained directly as follows.

Theorem 1. *The rational GT-Bernstein basis functions defined in (2) have the following properties:*

(a) *Nonnegativity.* $T_{a_i}(t) \geq 0, t \in \Delta_{\mathcal{A}}, i = 0, 1, \cdots, n$.
(b) *Partition of the unity.* $\sum_{i=0}^{n} T_{a_i}(t) \equiv 1$.
(c) *Normalized totally positive (NTP). The rational GT-Bernstein basis* $\{T_{a_i}(t)\}_{i=0}^{n}$ *is a NTP basis. This property is proved recently by Yu et al. [32].*
(d) *Endpoints property. At the endpoints of* $[a_0, a_n]$, *we have*

$$T_{a_i}(a_0) = \begin{cases} 1, & i = 0, \\ 0, & i \neq 0, \end{cases} \qquad T_{a_i}(a_n) = \begin{cases} 1, & i = n, \\ 0, & i \neq n. \end{cases}$$

(e) *Degeneration property. The GT-Bernstein basis* $\{\beta_{a_i}(t)\}$ *degenerates to the classical Bernstein basis for* $\mathcal{A} = \{0, 1, \cdots, n\}$ *or* $\mathcal{A} = \{0, \frac{1}{n}, \cdots, 1\}$ *after proper parameter transformation, and to toric-Bernstein basis for* $\mathcal{A} \subset \mathbb{Z}$. *Therefore, the rational GT-Bernstein basis degenerates to rational Bernstein basis for* $\mathcal{A} = \{0, 1, \cdots, n\}$ *or* $\mathcal{A} = \{0, \frac{1}{n}, \cdots, 1\}$ *after proper parameter transformation.*

Yu et al. [32] presented the following result for GT-Bernstein basis.

Theorem 2. *Suppose* $k_0 = k_1 = k$ *and set* $a_0 \leq t_0 < t_1 < \cdots < t_n \leq a_n$ *to be an any increasing sequence. Then the collocation matrix of* $\{\beta_{a_i}(t)\}_{i=0}^{n}$ *at* $t_0 < t_1 < \cdots < t_n$

$$M\begin{pmatrix} \beta_{a_0}, \cdots, \beta_{a_n} \\ t_0, \cdots, t_n \end{pmatrix} = (\beta_{a_j}(t_i))_{j=0,1,\cdots,n}^{i=0,1,\cdots,n} \tag{3}$$

is a strictly totally positive matrix.

Since the basis $\{\beta_{a_i}(t)\}_{i=0}^{n}$ defined by equation (1) may do not hold the property of partition of the unity on $\Delta_{\mathcal{A}}$ for arbitrary positive coefficients, we present a method to choose coefficients by Theorem 2, which makes the basis $\{\beta_{a_i}(t)\}$ has partition of the unity on a given increasing sequence $a_0 \le t_0 < t_1 < \cdots < t_n \le a_n$.

Given an increasing sequence $a_0 \le t_0 < t_1 < \cdots < t_n \le a_n$, we have the following system of equations:

$$\sum_{j=0}^{n} \beta_{a_j}(t_i) = c_{a_0} h_0(t_i)^{h_0(a_0)} h_1(t_i)^{h_1(a_0)} + \cdots + c_{a_n} h_0(t_i)^{h_0(a_n)} h_1(t_i)^{h_1(a_n)} = 1, \quad i = 0, \cdots, n. \tag{4}$$

If we write $\mathbf{C} = (c_{a_0}, \cdots, c_{a_n})^T$ and $\mathbf{1} = (1, \cdots, 1)^T$, then we obtain

$$M \begin{pmatrix} \beta_{a_0}, \cdots, \beta_{a_n} \\ t_0, \cdots, t_n \end{pmatrix} \mathbf{C} = \mathbf{1}. \tag{5}$$

It's clear that the basis $\{\beta_{a_i}(t)\}_{i=0}^{n}$ satisfies the conditions of Theorem 2, then the matrix M is a strictly totally positive matrix and system of equations (5) has a unique solution. For the bivariate generalized toric-Bernstein basis in Section 2.2, the method for selection of the coefficients is similar to the univariate case.

2.2 Bivariate generalized toric-Bernstein basis functions

Consider a finite set of real points $\mathcal{A} = \{\mathbf{a}_0, \mathbf{a}_1, \cdots, \mathbf{a}_n\} \subset \mathbb{R}^2$, Let $\Delta_{\mathcal{A}}$ be the convex hull of $\mathcal{A}$. The lines defined by edges ϕ_i of $\Delta_{\mathcal{A}}$ are $h_i(u, v) = \xi_i u + \eta_i v + \rho_i$, where $\langle \xi_i, \eta_i \rangle$ is the normal vector of ϕ_i towards inside of $\Delta_{\mathcal{A}}$ such that $h_i(u, v) \ge 0, (u, v) \in \Delta_{\mathcal{A}}, i = 1, \cdots, r$. We construct the generalized toric-Bernstein basis functions as follows.

Definition 2. *Let $\mathcal{A} = \{\mathbf{a}_0, \mathbf{a}_1, \cdots, \mathbf{a}_n\} \subset \mathbb{R}^2$ be a finite collection of real points, and set $\Delta_{\mathcal{A}}$ to be the convex hull of $\mathcal{A}$. Then, for any point $\mathbf{a}_i$ in $\mathcal{A}$, we define the bivariate generalized toric-Bernstein (GT-Bernstein) basis function as*

$$\beta_{\mathbf{a}_i}(u, v) = c_{\mathbf{a}_i} h_1(u, v)^{h_1(\mathbf{a}_i)} \cdots h_r(u, v)^{h_r(\mathbf{a}_i)}, \quad (u, v) \in \Delta_{\mathcal{A}}, \tag{6}$$

where $c_{\mathbf{a}_i} > 0$ is the coefficient and $\mathbf{a}_i$ is called knot.

The rational form of the GT-Bernstein basis function $\beta_{\mathbf{a}_i}(u, v)$ is

$$T_{\mathbf{a}_i}(u, v) = \frac{\omega_{\mathbf{a}_i} \beta_{\mathbf{a}_i}(u, v)}{\sum_{i=0}^{n} \omega_{\mathbf{a}_i} \beta_{\mathbf{a}_i}(u, v)}, \quad (u, v) \in \Delta_{\mathcal{A}}. \tag{7}$$

where $\omega_{\mathbf{a}_i} > 0$ is called weight.

Remark 2. *In (6), the basis function depends on the choice of coefficients, and the coefficients can vary from case to case. If there is no special explanation, we set $c_{\mathbf{a}_i} \equiv 1$.*

Example 2. *Let $\widetilde{\mathcal{A}} = \{(0, 2), (1, 2), (0, \frac{6}{5}), (\frac{8}{7}, \frac{8}{7}), (2, 1), (0, 0), (\frac{6}{5}, 0), (2, 0)\}$ (see Figure 1(b)). By (6), the GT-Bernstein basis defined by $\widetilde{\mathcal{A}}$ are given as belows*

$$\beta_{(0,2)}(u, v) = (3 - u - v)(2 - u)^2 v^2, \quad \beta_{(1,2)}(u, v) = (2 - u) v^2 u, \quad \beta_{(0,\frac{6}{5})}(u, v) = (2 - v)^{\frac{4}{5}} (3 - u - v)^{\frac{9}{5}} (2 - u)^2 v^{\frac{6}{5}},$$
$$\beta_{(\frac{8}{7},\frac{8}{7})}(u, v) = (2 - v)^{\frac{6}{7}} (3 - u - v)^{\frac{5}{7}} (2 - u)^{\frac{6}{7}} v^{\frac{8}{7}} u^{\frac{8}{7}}, \quad \beta_{(2,1)}(u, v) = (2 - v) v u^2, \quad \beta_{(0,0)}(u, v) = (2 - v)^2 (3 - u - v)^3 (2 - u)^2,$$
$$\beta_{(\frac{6}{5},0)}(u, v) = (2 - v)^2 (3 - u - v)^{\frac{9}{5}} (2 - u)^{\frac{4}{5}} u^{\frac{6}{5}}, \quad \beta_{(2,0)}(u, v) = (2 - v)^2 (3 - u - v) u^2.$$

Three of the basis functions are shown in Figure 5. We further set each weight $\omega_{\mathbf{a}_i} = 1$, then the rational forms of these three basis functions on $\Delta_{\mathcal{A}}$ are shown in Figure 6.

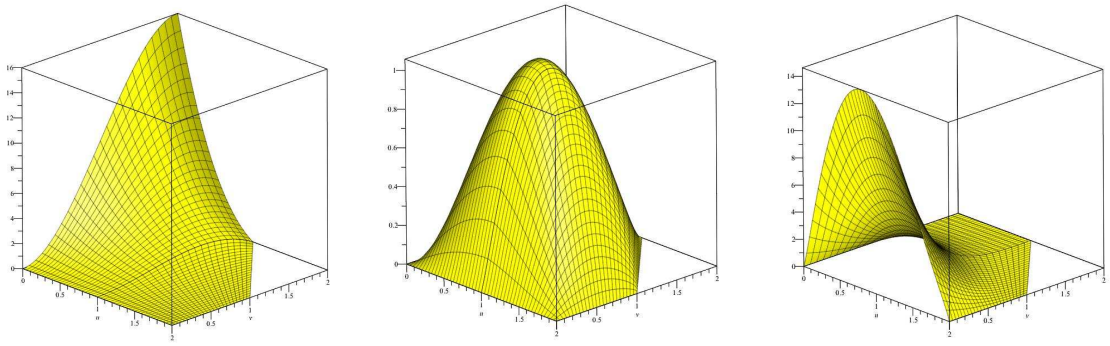

(a) $\beta_{(0,2)}(u,v)$ (b) $\beta_{(\frac{8}{7},\frac{8}{7})}(u,v)$ (c) $\beta_{(\frac{6}{5},0)}(u,v)$

Figure 5: GT-Bernstein basis functions.

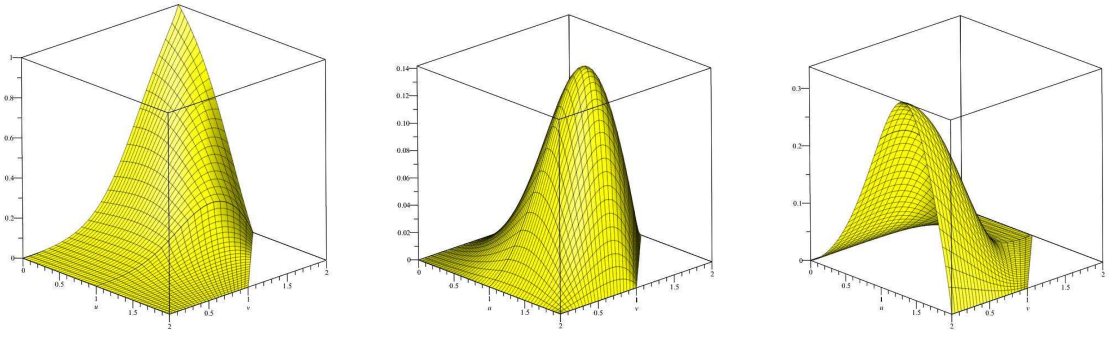

(a) $T_{(0,2)}(u,v)$ (b) $T_{(\frac{8}{7},\frac{8}{7})}(u,v)$ (c) $T_{(\frac{6}{5},0)}(u,v)$

Figure 6: Rational GT-Bernstein basis functions.

Suppose edges $\phi_i (i = 1, \cdots, r)$ of the convex hull $\Delta_{\mathcal{A}}$ are ordered counterclockwise and let V_i be vertex of $\Delta_{\mathcal{A}}$ where two edges ϕ_i and ϕ_{i+1} meet, $(i = 1, \cdots, r)$. The indices will be treated in a cyclic fashion: for instance, $\phi_0 = \phi_r$, $\phi_{r+1} = \phi_1$ and so on. Denote by $\hat{\phi}_i = \phi_i \cap \mathcal{A}$ the intersection of $\mathcal{A}$ and ϕ_i. Note that $\{V_i\}_{i=1}^r$ and $\hat{\phi}_i$ are subsets of $\mathcal{A}$ respectively, $i = 1, \cdots, r$.

From Definition 2 and rational form (7), we can obtain the following properties of the basis functions $\{T_{\mathbf{a}_i}(u,v)\}$ directly.

Theorem 3. *The rational forms of the GT-Bernstein basis functions defined in (7) have the following properties:*

(a) *Nonnegativity.* $T_{\mathbf{a}_i}(u,v) \geq 0, (u,v) \in \Delta_{\mathcal{A}}, i = 0, 1, \cdots, n.$

(b) *Partition of the unity.* $\sum_{i=0}^{n} T_{\mathbf{a}_i}(u,v) \equiv 1.$

(c) *Boundary property. When* (u,v) *is constrained on the edge* ϕ_j *of* $\Delta_{\mathcal{A}}$*, all basis functions* $\beta_{\mathbf{a}_i}(u,v)$ *and* $T_{\mathbf{a}_i}(u,v)$ *with indices* $\mathbf{a}_i \in \mathcal{A} \setminus \hat{\phi}_j$ *vanish, that is:*

$$\begin{cases} \beta_{\mathbf{a}_i}(u,v) = 0, \ \mathbf{a}_i \in \mathcal{A} \setminus \hat{\phi}_j, \\ \qquad\qquad\qquad\qquad (u,v) \in \phi_j, \\ \beta_{\mathbf{a}_i}(u,v) \neq 0, \ \mathbf{a}_i \in \hat{\phi}_j, \end{cases}$$
$$\begin{cases} T_{\mathbf{a}_i}(u,v) = 0, \ \mathbf{a}_i \in \mathcal{A} \setminus \hat{\phi}_j, \\ \qquad\qquad\qquad\qquad (u,v) \in \phi_j. \\ T_{\mathbf{a}_i}(u,v) \neq 0, \ \mathbf{a}_i \in \hat{\phi}_j, \end{cases} \tag{8}$$

(d) *Corner points property. At the vertices of $\Delta_{\mathcal{A}}$, we have*

$$\begin{cases} T_{\mathbf{a}_i}(V_i) = 1, \ \mathbf{a}_i = V_i, \\ T_{\mathbf{a}_i}(V_i) = 0, \ \mathbf{a}_i \neq V_i. \end{cases} \tag{9}$$

(e) *Degeneration property. For $\mathcal{A} = \{\mathbf{a}_0, \mathbf{a}_1, \cdots, \mathbf{a}_n\} \subset \mathbb{Z}^2$, the basis defined by (6) degenerates into toric-Bernstein basis defined in [5]. In particular, the GT-Bernstein basis degenerates to the bivariate triangular Bernstein basis for $\mathcal{A} = \{(i, j) \in \mathbb{Z}^2 \mid i + j \leq k, i \geq 0, j \geq 0\}$, and to the tensor product Bernstein basis for $\mathcal{A} = \{(i, j) \in \mathbb{Z}^2 \mid 0 \leq i \leq m, 0 \leq j \geq n\}$, if coefficients selected properly.*

3 Generalized toric-Bézier curves

For given control points and weights, we can use the Bernstein basis functions to construct the classical rational Bézier curve. The classical rational Bézier curve has many good properties, such as convex hull property, boundary property, and affine invariance. In the same way, the basis functions defined by (2) can be used to define a new class of rational curves.

Definition 3. *Given real points set $\mathcal{A} = \{a_0, a_1, \cdots, a_n\}$, control points $\mathcal{B} = \{\mathbf{b}_{a_i} \mid a_i \in \mathcal{A}\} \subset \mathbb{R}^3$, and weights $\omega = \{\omega_{a_i} > 0 \mid a_i \in \mathcal{A}\}$, the rational parametric curve*

$$\mathbf{P}_{\mathcal{A},\omega,\mathcal{B}}(t) = \sum_{i=0}^{n} \mathbf{b}_{a_i} T_{a_i}(t) = \sum_{i=0}^{n} \mathbf{b}_{a_i} \frac{\omega_{a_i} \beta_{a_i}(t)}{\sum_{i=0}^{n} \omega_{a_i} \beta_{a_i}(t)}, \quad t \in \Delta_{\mathcal{A}} \tag{10}$$

is called the generalized toric-Bézier curve (GT-Bézier curve for short) of degree n.The n-edge polyline polygon is obtained by sequentially connecting two adjacent control points of $\mathcal{B}$ with a straight line segment, is called control polygon.

Remark 3. *Although the GT-Bernstein basis defined by equation (1) depends on the selection of the coefficients k_0 and k_1, the GT-Bézier curve is independent on the choice of these two parameters. It can be known from the results in [27], the GT-Bézier curve defined by the equation (10) is obtained by the projection (the projection is related to the weights and the control points) of the high-dimensional real projective toric variety defined by the $\mathcal{A} = \{a_0, a_1, \cdots, a_n\}$. Given point set $\mathcal{A}$, for different coefficients k_0 and k_1, after unitizing the corresponding toric variety and eliminating the constant in the projective space, the toric varieties are identical, then the GT-Bézier curve defined by point set $\mathcal{A}$ is also the same. For more Details refer to [6, 27].*

The degree of n of curve in Definition 3 is just the number of forms in the curve, one less than the number of knots of $\mathcal{A}$, not exactly the polynomial degree of curve in general sense. If $\mathcal{A} \subset \mathbb{Z}$, then this degree is exactly the polynomial degree of curve .

Example 3. *Let $\mathcal{A} = \{a_0 = 0, a_1 = \frac{\sqrt{2}}{4}, a_2 = \frac{1}{2}, a_3 = \frac{\sqrt{2}}{2}, a_4 = 1\}$ as show in Example 1 , weights $\omega_{a_0} = 1, \omega_{a_1} = 10, \omega_{a_2} = 20, \omega_{a_3} = 6, \omega_{a_4} = 5$ and control points $\mathbf{b}_{a_0} = (0, 0), \mathbf{b}_{a_1} = (0.4, 1.3), \mathbf{b}_{a_2} = (2, 2), \mathbf{b}_{a_3} = (3.7, 1.5), \mathbf{b}_{a_4} = (4, 0)$. Suppose $c_{a_i} = 1 (i = 0, \cdots, 4)$, then the quadratic GT-Bézier curve is*

$$\mathbf{P}_{\mathcal{A},\omega,\mathcal{B}}(t) = \sum_{i=0}^{4} \mathbf{b}_{a_i} T_{a_i}(t), \ t \in [0, 1],$$

and the curve is shown in Figure 7.

From the properties of the GT-Bernstein basis functions associated with $\mathcal{A} = \{a_0, a_1, \cdots, a_n\} \subset \mathbb{R}$, some properties of the GT-Bézier curve can be obtained as follows:

(a) Affine invariance and convex hull property. Since the basis (2) have the properties of nonnegativity and partition of the unity, these show that the corresponding GT-Bézier curve (10) has affine invariance and convex hull property.

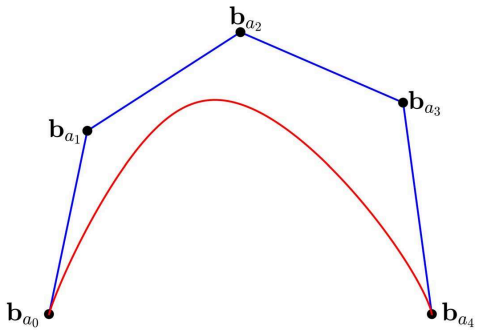

Figure 7: Quadratic GT-Bézier curve.

(b) Endpoints interpolation property. This property follows directly from the endpoints property of the basis (2), that is $\mathbf{P}_{\mathcal{A},\omega,\mathcal{B}}(a_0) = \mathbf{b}_{a_0}$, $\mathbf{P}_{\mathcal{A},\omega,\mathcal{B}}(a_n) = \mathbf{b}_{a_n}$.

(c) Progressive iteration approximation (PIA) property. The GT-Bézier curve has PIA property from the result in [31] because its basis $\{T_{a_i}(t)\}_{i=0}^{n}$ is a NTP basis.

(d) Degeneration property. If $a_i = i$ (or $a_i = \frac{i}{n}$), $(i = 0, 1, \cdots, n)$ and $k_0 = k_1 = n$, then the GT-Bézier curve (10) degenerates into the classical rational Bézier curve after reparameterization and coefficients selected properly. For $\mathcal{A} = \{a_0, a_1, \cdots, a_n\} \subset \mathbb{Z}$, the GT-Bézier curve (10) is the toric Bézier curve defined in [33], which is exactly the one-dimensional form of the toric surface defined in [5].

(e) Endpoints tangent vectors. For

$$k_0 = \frac{1}{a_1 - a_0}, k_1 = \frac{1}{a_n - a_{n-1}},$$

the tangent vectors at the end points of GT-Bézier curve are

$$\begin{aligned}\mathbf{P}'_{\mathcal{A},\omega,\mathcal{B}}(a_0)&=\frac{c_{a_1}k_0k_1^{-\frac{k_1}{k_0}}(a_n-a_0)^{-\frac{k_1}{k_0}}\omega_{a_1}(\mathbf{b}_{a_1}-\mathbf{b}_{a_0})}{c_{a_0}\omega_{a_0}},\\ \mathbf{P}'_{\mathcal{A},\omega,\mathcal{B}}(a_n)&=\frac{c_{a_{n-1}}k_1k_0^{-\frac{k_0}{k_1}}(a_n-a_0)^{-\frac{k_0}{k_1}}\omega_{a_{n1}}(\mathbf{b}_{a_n}-\mathbf{b}_{a_{n-1}})}{c_{a_n}\omega_{a_n}}.\end{aligned} \tag{11}$$

We can see the tangent vectors at the end points of curve $\mathbf{P}_{\mathcal{A},\omega,\mathcal{B}}(t)$ are parallel to $\overrightarrow{\mathbf{b}_{a_0}\mathbf{b}_{a_1}}$ and $\overrightarrow{\mathbf{b}_{a_{n-1}}\mathbf{b}_{a_n}}$ respectively. And this property can be used to construct G^1 continuous piecewise GT-Bézier curve.

(f) Multiple knot property. When a knot in $\mathcal{A}$ tends to its adjacent knot, the following results describe the limit property of the GT-Bézier curve, which also show the resulting GT-Bézier curve defined by $\mathcal{A}$ with multiple knots.

Theorem 4. *Suppose $c_{a_i} = 1 (i = 0, \cdots, n)$. When knot a_k $(0 \le k < n)$ approaches to its adjacent knot a_{k+1}, the limit of GT-Bézier curve $\mathbf{P}_{\mathcal{A},\omega,\mathcal{B}}(t)$ of degree n defined in (10) is exactly the GT-Bézier curve $\widetilde{\mathbf{P}}_{\widetilde{\mathcal{A}},\widetilde{\omega},\widetilde{\mathcal{B}}}(t)$ of degree $n-1$, defined as*

$$\lim_{a_k\to a_{k+1}}\mathbf{P}_{\mathcal{A},\omega,\mathcal{B}}(t)=\widetilde{\mathbf{P}}_{\widetilde{\mathcal{A}},\widetilde{\omega},\widetilde{\mathcal{B}}}(t)=\frac{\sum_{i=0}^{k-1}\omega_{a_i}\mathbf{b}_{a_i}\beta_{a_i}(t)+\widetilde{\omega}_{a_{k+1}}\widetilde{\mathbf{b}}_{a_{k+1}}\beta_{a_{k+1}}(t)+\sum_{i=k+2}^{n}\omega_{a_i}\mathbf{b}_{a_i}\beta_{a_i}(t)}{\sum_{i=0}^{k-1}\omega_{a_i}\beta_{a_i}(t)+\widetilde{\omega}_{a_{k+1}}\beta_{a_{k+1}}(t)+\sum_{i=k+2}^{n}\omega_{a_i}\beta_{a_i}(t)}, \tag{12}$$

where

$$\widetilde{\omega}_{a_{k+1}}=\omega_{a_k}+\omega_{a_{k+1}},\quad \widetilde{\mathbf{b}}_{a_{k+1}}=\frac{\omega_{a_k}}{\omega_{a_k}+\omega_{a_{k+1}}}\mathbf{b}_{a_k}+\frac{\omega_{a_{k+1}}}{\omega_{a_k}+\omega_{a_{k+1}}}\mathbf{b}_{a_{k+1}},$$

$$\widetilde{\mathcal{A}}=\{a_0,\cdots,a_{k-1},a_{k+1},\cdots,a_n\},\quad \widetilde{\mathcal{B}}=\{\mathbf{b}_{a_0},\cdots,\mathbf{b}_{a_{k-1}},\widetilde{\mathbf{b}}_{a_{k+1}},\mathbf{b}_{a_{k+2}},\cdots,\mathbf{b}_{a_n}\},$$
$$\widetilde{\omega}=\{\omega_{a_0},\cdots,\omega_{a_{k-1}},\widetilde{\omega}_{a_{k+1}},\omega_{a_{k+2}},\cdots,\omega_{a_n}\}.$$

Proof. When a_k $(0 \le k < n)$ tends to a_{k+1}, we have

$$\lim_{a_k\to a_{k+1}}\beta_{a_k}(t)=\lim_{a_k\to a_{k+1}}(t-a_0)^{a_k-a_0}(a_n-t)^{a_n-a_k}=(t-a_0)^{a_{k+1}-a_0}(a_n-t)^{a_n-a_{k+1}}=\beta_{a_{k+1}}(t).$$

Thus,

$$\begin{aligned}\lim_{a_k\to a_{k+1}}\sum_{i=0}^{n}\mathbf{b}_{a_i}T_{a_i}(t)=\widetilde{\mathbf{P}}_{\widetilde{\mathcal{A}},\widetilde{\omega},\widetilde{\mathcal{B}}}(t)&=\lim_{a_k\to a_{k+1}}\sum_{i=0}^{n}\frac{\mathbf{b}_{a_i}\omega_{a_i}\beta_{a_i}(t)}{\sum_{i=0}^{n}\omega_{a_i}\beta_{a_i}(t)}\\&=\frac{\sum_{i\neq k,k+1}\omega_{a_i}\mathbf{b}_{a_i}\beta_{a_i}(t)+\omega_{a_k}\mathbf{b}_{a_k}\beta_{a_{k+1}}(t)+\omega_{a_{k+1}}\mathbf{b}_{a_{k+1}}\beta_{a_{k+1}}(t)}{\sum_{i\neq k,k+1}\omega_{a_i}\beta_{a_i}(t)+\omega_{a_k}\beta_{a_{k+1}}(t)+\omega_{a_{k+1}}\beta_{a_{k+1}}(t)}\\&=\frac{\sum_{i\neq k,k+1}\omega_{a_i}\mathbf{b}_{a_i}\beta_{a_i}(t)+(\omega_{a_k}\mathbf{b}_{a_k}+\omega_{a_{k+1}}\mathbf{b}_{a_{k+1}})\beta_{a_{k+1}}(t)}{\sum_{i\neq k,k+1}\omega_{a_i}\beta_{a_i}(t)+(\omega_{a_k}+\omega_{a_{k+1}})\beta_{a_{k+1}}(t)}.\end{aligned}$$

Let $\widetilde{\omega}_{a_{k+1}}=\omega_{a_k}+\omega_{a_{k+1}}$, $\widetilde{\mathbf{b}}_{a_{k+1}}=\frac{\omega_{a_k}}{\omega_{a_k}+\omega_{a_{k+1}}}\mathbf{b}_{a_k}+\frac{\omega_{a_{k+1}}}{\omega_{a_k}+\omega_{a_{k+1}}}\mathbf{b}_{a_{k+1}}$, we can obtain

$$\lim_{a_k\to a_{k+1}}\mathbf{P}_{\mathcal{A},\omega,\mathcal{B}}(t)=\widetilde{\mathbf{P}}_{\widetilde{\mathcal{A}},\widetilde{\omega},\widetilde{\mathcal{B}}}(t)=\frac{\sum_{i\neq k,k+1}\omega_{a_i}\mathbf{b}_{a_i}\beta_{a_i}(t)+\widetilde{\omega}_{a_{k+1}}\widetilde{\mathbf{b}}_{a_{k+1}}\beta_{a_{k+1}}(t)}{\sum_{i\neq k,k+1}\omega_{a_i}\beta_{a_i}(t)+\widetilde{\omega}_{a_{k+1}}\beta_{a_{k+1}}(t)},$$

where

$$\widetilde{\mathcal{A}}=\{a_0,\cdots,a_{k-1},a_{k+1},\cdots,a_n\},\quad \widetilde{\mathcal{B}}=\{\mathbf{b}_{a_0},\cdots,\mathbf{b}_{a_{k-1}},\widetilde{\mathbf{b}}_{a_{k+1}},\mathbf{b}_{a_{k+2}},\cdots,\mathbf{b}_{a_n}\},$$
$$\widetilde{\omega}=\{\omega_{a_0},\cdots,\omega_{a_{k-1}},\widetilde{\omega}_{a_{k+1}},\omega_{a_{k+2}},\cdots,\omega_{a_n}\}.$$

This leads to prove the result. □

Example 4. *Consider the curve* $\mathbf{P}_{\mathcal{A},\omega,\mathcal{B}}(t)$ *defined as in Example 3. Let knots* $\mathcal{A}=\{a_0=0,a_1=\frac{\sqrt{2}}{4},a_2=\frac{1}{2},a_3=\frac{\sqrt{2}}{2},a_4=1\}$, *weights* $\omega_{a_0}=1,\omega_{a_1}=10,\omega_{a_2}=20,\omega_{a_3}=6,\omega_{a_4}=5$, *control points* $\mathbf{b}_{a_0}=(0,0),\mathbf{b}_{a_1}=(0.4,1.3),\mathbf{b}_{a_2}=(2,2),\mathbf{b}_{a_3}=(3.7,1.5),\mathbf{b}_{a_4}=(4,0)$ *and* $c_{a_i}=1$ $(i=0,\cdots,4)$. *If* a_1 *approaches* a_2, *then the changes of the GT-Bézier curve are shown in Figure 8. We can see that the limit curve* $\lim_{a_1\to a_2}\mathbf{P}_{\mathcal{A},\omega,\mathcal{B}}(t)$ *coincides with the target curve* $\widetilde{\mathbf{P}}_{\widetilde{\mathcal{A}},\widetilde{\omega},\widetilde{\mathcal{B}}}(t)$, *which verifies the Theorem 4.*

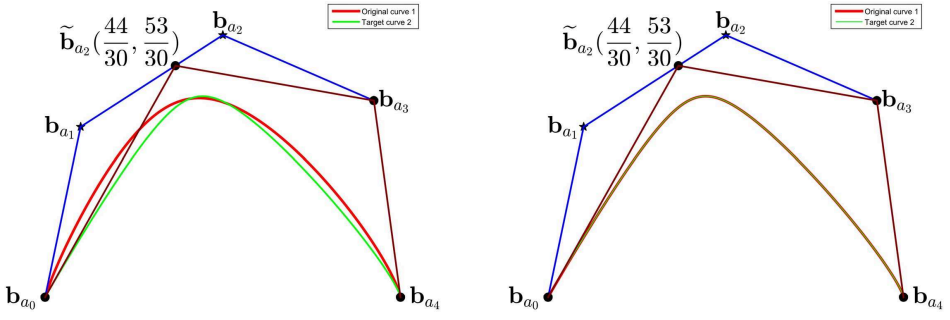

(a) Initial curve (b) Limit curve

Figure 8: Limits of the quadratic GT-Bézier curve of single knot.

Theorem 4 indicates that the GT-Bézier curve of degree n degenerates into the GT-Bézier curve of degree $n-1$ with knots $\widetilde{\mathcal{A}}=\{a_0,\cdots,a_{k-1},a_{k+1},\cdots,a_n\}$, control points $\widetilde{\mathcal{B}}=\{\mathbf{b}_{a_0},\cdots,\mathbf{b}_{a_{k-1}},\widetilde{\mathbf{b}}_{a_{k+1}},\mathbf{b}_{a_{k+2}},\cdots,\mathbf{b}_{a_n}\}$

and weights $\widetilde{\omega} = \{\omega_{a_0}, \cdots, \omega_{a_{k-1}}, \widetilde{\omega}_{a_{k+1}}, \omega_{a_{k+2}}, \cdots, \omega_{a_n}\}$ when $a_k = a_{k+1}$. The following corollary generalizes Theorem 4, and gives the limit of GT-Bézier curve with multiple knots. The proof of the corollary is similar to Theorem 4 and will be omitted here.

Corollary 1. *Suppose $c_{a_i} = 1\ (i = 0, \cdots, n)$. When knots $a_q, a_{q+1}, \cdots, a_{q+k-2} (0 \le q < n, 1 < k \le n+1-q)$ approaches to the knot a_{q+k-1}, the limit of GT-Bézier curve $\mathbf{P}_{\mathcal{A},\omega,\mathcal{B}}(t)$ of degree n defined in (10) is exactly the GT-Bézier curve of degree $n-k+1$ as*

$$\lim_{a_q,\cdots,a_{q+k-2}\to a_{q+k-1}} \mathbf{P}_{\mathcal{A},\omega,\mathcal{B}}(t) = \widetilde{\mathbf{P}}_{\widetilde{\mathcal{A}},\widetilde{\omega},\widetilde{\mathcal{B}}}(t) = \frac{\sum_{i=0}^{q-1} \omega_{a_i}\mathbf{b}_{a_i}\beta_{a_i}(t) + \widetilde{\omega}_{a_{q+k-1}}\widetilde{\mathbf{b}}_{a_{q+k-1}}\beta_{a_{q+k-1}}(t) + \sum_{i=q+k}^{n} \omega_{a_i}\mathbf{b}_{a_i}\beta_{a_i}(t)}{\sum_{i=0}^{q-1} \omega_{a_i}\beta_{a_i}(t) + \widetilde{\omega}_{a_{q+k-1}}\beta_{a_{q+k-1}}(t) + \sum_{i=q+k}^{n} \omega_{a_i}\beta_{a_i}(t)},$$

where

$$\widetilde{\omega}_{a_{q+k-1}} = \omega_{a_q} + \omega_{a_{q+1}} + \cdots + \omega_{a_{q+k-1}}, \quad \widetilde{\mathbf{b}}_{a_{q+k-1}} = \frac{\omega_{a_q}}{\widetilde{\omega}_{a_{q+k-1}}}\mathbf{b}_{a_q} + \cdots + \frac{\omega_{a_{q+k-1}}}{\widetilde{\omega}_{a_{q+k-1}}}\mathbf{b}_{a_{q+k-1}},$$

$$\widetilde{\mathcal{A}} = \{a_0, \cdots, a_{q-1}, a_{q+k-1}, \cdots, a_n\}, \quad \widetilde{\mathcal{B}} = \{\mathbf{b}_{a_0}, \cdots, \mathbf{b}_{a_{q-1}}, \widetilde{\mathbf{b}}_{a_{q+k-1}}, \mathbf{b}_{a_{q+k}}, \cdots, \mathbf{b}_{a_n}\},$$

$$\widetilde{\omega} = \{\omega_{a_0}, \cdots, \omega_{a_{q-1}}, \widetilde{\omega}_{a_{q+k-1}}, \omega_{a_{q+k}}, \cdots, \omega_{a_n}\}.$$

Example 5. *Consider the curve $\mathbf{P}_{\mathcal{A},\omega,\mathcal{B}}(t)$ defined as in Example 3. If $a_1 \to a_2$ and $a_3 \to a_2$, then the changes of the GT-Bézier curve are shown in Figure 9. The limit curve is constructed by knots $\widetilde{\mathcal{A}} = \{a_0 = 0, a_2 = \frac{1}{2}, a_4 = 1\}$, control points $\widetilde{\mathcal{B}} = \{\mathbf{b}_{a_0} = (0,0), \widetilde{\mathbf{b}}_{a_2} = (\frac{66.2}{36}, \frac{62}{36}), \mathbf{b}_{a_4} = (4,0)\}$ and weights $\widetilde{\omega} = \{\omega_{a_0} = 1, \widetilde{\omega}_{a_2} = 36, \omega_{a_4} = 5\}$. We can see that the limit curve coincides with the target curve together, which verifies the result of Corollary 1.*

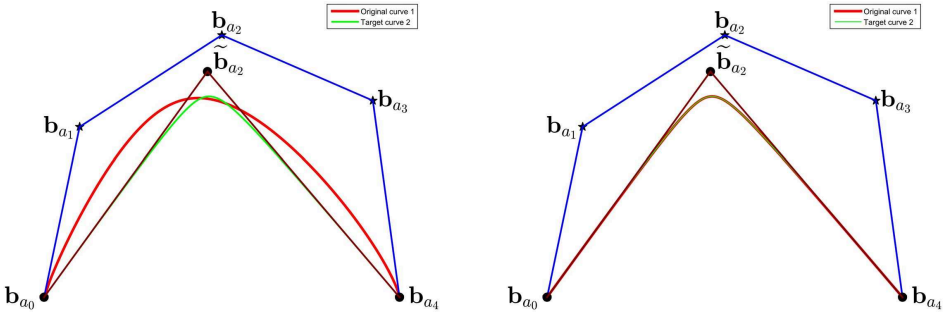

(a) Initial curve (b) Limit curve

Figure 9: Limits of the quadratic GT-Bézier curve with multiple knots.

(g) Toric degeneration property. For each $t \in \Delta_{\mathcal{A}}$, we have the limiting property of GT-Bézier curve while a single weight of curve tends to infinity, that is

$$\lim_{\omega_{a_i}\to+\infty} \mathbf{P}_{\mathcal{A},\omega,\mathcal{B}}(t) = \begin{cases} \mathbf{b}_{a_0} & t = a_0, \\ \mathbf{b}_{a_i} & t \in (a_0, a_n), \\ \mathbf{b}_{a_n} & t = a_n. \end{cases}$$

And this property can be derived from weight property of rational Bézier curve directly. Figure 10 shows the limit curve of GT-Bézier curve defined in Example 3 with $\omega_{a_1} \to +\infty$.

Next, we consider the property of GT-Bézier curve if all the weights tend to infinity.

Let $\lambda : \mathcal{A} \to \mathbb{R}$ be a lifting function to lift the points a_i of $\mathcal{A}$ to $(a_i, \lambda(a_i)) \in \mathbb{R}^2$. We denote $P_\lambda = conv\{(a_i, \lambda(a_i)) \mid a_i \in \mathcal{A}\}$ the convex hull of the lifted points. Each edge of the convex hull P_λ has a

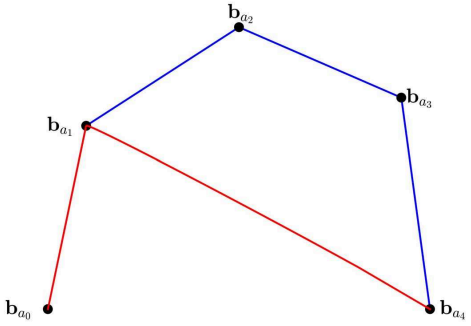

Figure 10: Limit of GT-Bézier curve with $\omega_{a_1} \to +\infty$.

normal vector pointing to the outer side. We call it the upper edges of P_λ if the last coordinate of the normal vector is positive. If we project these upper edges back vertically into $\mathbb{R}$, they can cover $\Delta_{\mathcal{A}}$ and form a regular subdivision Γ_λ of $\Delta_{\mathcal{A}}$ induced by λ [6].

We group together the points of $\mathcal{A}$ that are in the same subset of the Γ_λ and on the same upper edge of the P_λ. Then we get a decomposition of $\mathcal{A}$, which is called regular decomposition $\mathcal{S}_\lambda$ of $\mathcal{A}$ induced by λ. For each subset $\mathcal{F}$ of $\mathcal{S}_\lambda$, we can use the weights $\omega|_{\mathcal{F}} = \{\omega_{a_i} \mid a_i \in \mathcal{F}\}$ and the control points $\mathcal{B}|_{\mathcal{F}} = \{\mathbf{b}_{a_i} \mid a_i \in \mathcal{F}\}$ to define a new GT-Bézier curve $\mathbf{P}_{\mathcal{F},\omega|_{\mathcal{F}},\mathcal{B}|_{\mathcal{F}}}$ on $\Delta_{\mathcal{F}} = conv\{a_i \in \mathcal{F} \mid a_i \in \mathcal{A}\}$ by Definition 3. The union of these curves

$$\mathbf{P}_{\mathcal{A},\omega,\mathcal{B}}(\mathcal{S}_\lambda) = \bigcup_{\mathcal{F}\in\mathcal{S}_\lambda} \mathbf{P}_{\mathcal{F},\omega|_{\mathcal{F}},\mathcal{B}|_{\mathcal{F}}}$$

is called the regular control curve of $\mathbf{P}_{\mathcal{A},\omega,\mathcal{B}}$ induced by regular decomposition $\mathcal{S}_\lambda$.

We can use lifting function λ to get a set of weights with a parameter x, $\omega_\lambda(x) := \{x^{\lambda(a_i)}\omega_{a_i} \mid a_i \in \mathcal{A}\}$. These weights are used to define the map

$$\mathbf{P}_{\mathcal{A},\omega_\lambda(x),\mathcal{B}}(t) = \frac{\sum_{i=0}^{n} x^{\lambda(a_i)}\omega_{a_i}\mathbf{b}_{a_i}\beta_{a_i}(t)}{\sum_{i=0}^{n} x^{\lambda(a_i)}\omega_{a_i}\beta_{a_i}(t)}, \quad t \in \Delta_{\mathcal{A}}. \tag{13}$$

The image of $\Delta_{\mathcal{A}}$ under this map is a GT-Bézier curve with a parameter x, denoted as $P_{\mathcal{A},\omega_\lambda(x),\mathcal{B}}$. We have the following result.

Theorem 5. *The limit of the GT-Bézier curve $\mathbf{P}_{\mathcal{A},\omega_\lambda(x),\mathcal{B}}$ as $x \to \infty$ is the regular control curve induced by regular decomposition $\mathcal{S}_\lambda$, that is*

$$\lim_{x\to\infty} \mathbf{P}_{\mathcal{A},\omega_\lambda(x),\mathcal{B}} = \mathbf{P}_{\mathcal{A},\omega,\mathcal{B}}(\mathcal{S}_\lambda).$$

Proof. According to the theory of real irrational toric varieties in [27], the GT-Bézier curve $\mathbf{P}_{\mathcal{A},\omega,\mathcal{B}}$ is obtained by the projection of the high-dimensional real projective toric variety formed by $\mathcal{A}$. Then $\mathbf{P}_{\mathcal{A},\omega,\mathcal{B}}$ is projection after the composition of a sequence of mappings

$$\mathcal{A} \xrightarrow{\{\beta_{a_i}|a_i\in\mathcal{A}\}} X_{\mathcal{A}} \xrightarrow{\omega} X_{\mathcal{A},\omega} \xrightarrow{\mathcal{B}} \mathbf{P}_{\mathcal{A},\omega,\mathcal{B}}.$$

For $\mathcal{A}$ and weights $\omega_\lambda(x)$ with parameter x, we can get a family of translated toric varieties $X_{\mathcal{A},\omega_\lambda(x)}$

$$\mathcal{A} \xrightarrow{\{\beta_{a_i}|a_i\in\mathcal{A}\}} X_{\mathcal{A}} \xrightarrow{\omega_\lambda(x)} X_{\mathcal{A},\omega_\lambda(x)}.$$

When $x \to \infty$, $X_{\mathcal{A},\omega_\lambda(x)}$ limits to a union of irrational toric varieties in the Hausdorff distance, which are defined by the all of subset of $\mathcal{S}_\lambda$. That is

$$\lim_{x\to\infty} X_{\mathcal{A},\omega_\lambda(x)} = \bigcup_{\mathcal{F}\in\mathcal{S}_\lambda} X_{\mathcal{F},\omega|_{\mathcal{F}}}.$$

Then add control points $\mathcal{B}$, we have

$$\bigcup_{\mathcal{F}\in\mathcal{S}_\lambda} X_{\mathcal{F},\omega|_{\mathcal{F}}} \xrightarrow{\mathcal{B}} \bigcup_{\mathcal{F}\in\mathcal{S}_\lambda} \mathbf{P}_{\mathcal{F},\omega|_{\mathcal{F}},\mathcal{B}|_{\mathcal{F}}} = \mathbf{P}_{\mathcal{A},\omega,\mathcal{B}}(\mathcal{S}_\lambda).$$

So the result holds. □

Theorem 5 shows that regular control curves are exactly the limits of the GT-Bézier curve when all the weights tend to infinity. Obviously the control polygon is the regular control curve of GT-Bézier curve. This property is also called toric degeneration of GT-Bézier curves.

Example 6. *Let* $\mathcal{A} = \{0, \frac{\sqrt{2}}{4}, \frac{1}{2}, \frac{\sqrt{2}}{2}, 1\}$*, and the lifted values of* $\mathcal{A}$ *by a lifting function* λ *be* $(2, 1, 5, 9 - 4\sqrt{2}, 1)$*. This induces a regular decomposition of* $\mathcal{A}$ *as*

$$\left\{\{0, \frac{1}{2}\}, \{\frac{1}{2}, \frac{\sqrt{2}}{2}, 1\}\right\}.$$

The lifted point $\frac{\sqrt{2}}{4}$ *doesn't lie on any upper edge of the lifting polygon* P_λ*,then it doesn't lie on any subset of the decomposition.*

Figure 11(a) shows $\mathcal{A}$*, the lifted values of* $\mathcal{A}$ *by* λ*, and the corresponding regular decomposition. Figure 11(b) and 11(c) show the toric degeneration of this GT-Bézier curve for* $x = 2$*, and* $x = 3$*. The GT-Bézier curve approaches its regular control curve as the parameter x becomes larger.*

If λ' *takes the values of* $\mathcal{A}$ *as* $\{0, 2.5, 3, 2.5, 0\}$*, then this induces a regular decomposition of* $\mathcal{A}$ *as*

$$\left\{\{0, \frac{\sqrt{2}}{4}\}, \{\frac{\sqrt{2}}{4}, \frac{1}{2}\}, \{\frac{1}{2}, \frac{\sqrt{2}}{2}\}, \{\frac{\sqrt{2}}{2}, 1\}\right\}.$$

The corresponding regular decomposition is shown in Figure 12(a) and the regular control curve is exactly the control polygon of the curve.

Moreover λ'' *takes the values of* $\mathcal{A}$ *as* $\{1, 3, 1, 0, 1\}$*, then the regular decomposition of* $\mathcal{A}$ *is* $\left\{\{0,\frac{\sqrt{2}}{4}\},\{\frac{\sqrt{2}}{4},1\}\right\}$ *(see Figure 12(b)) and the regular control curve is as shown in Figure 10.*

(h) Variation diminishing (VD) property. Let $d_i = a_i - a_0$ $(i = 1, \cdots, n)$ for $\mathcal{A} = \{a_0, a_1, \cdots, a_n\} \subset \mathbb{R}$ with $a_0 \le a_1 \le \cdots \le a_{n-1} \le a_n$. If d_i $(i = 1, \cdots, n)$ are rational numbers, then d_i can be expressed as $d_i = \frac{p_i}{q_i}(p_i, q_i \in \mathbb{N})$. Let q be the least common multiple of $q_1, q_2, \cdots, q_n$, namely, $q = [q_1, q_2, \cdots, q_n]$, then $qd_i \in \mathbb{N} \setminus \{0\}$. At this point, we have the following theorem.

Theorem 6. *If* $d_i = a_i - a_0 \in \mathbb{Q}$ $(i = 1, 2, \cdots, n)$*, then the planar GT-Bézier curve* $\mathbf{P}_{\mathcal{A},\omega,\mathcal{B}}(t)$ *is variation diminishing, which means that the number of intersections of any straight line with the GT-Bézier curve* $\mathbf{P}_{\mathcal{A},\omega,\mathcal{B}}(t)$ *is no more than the number of intersections of the line with its control polygon.*

Proof. In order to prove this theorem, we need to use the Cartesian notation rule, which presents the upper bound of the number of the positive roots of the polynomial. For any polynomial $f(t) = m_0 + m_1 t + \cdots + m_n t^n$, if we write $Z_{t>0}[f(t)]$ to denote the number of positive roots of $f(t)$ and denote $V[m_0, m_1, \cdots, m_n]$ as the number of strict sign changes of polynomial coefficients, then

$$Z_{t>0}[m_0 + m_1 t + \cdots + m_n t^n] \le V[m_0, m_1, \cdots, m_n].$$

Let L denote any straight line, C denote the planar GT-Bézier curve defined by $\mathcal{A}$, and write $I(C, L)$ to denote the number of times L crosses C. Establish the Cartesian coordinate system with L as the abscissa axis. Because GT-Bézier curve is geometric invariant, we can let $(x_{a_i}, y_{a_i})(i = 0, 1, \cdots, n)$ represent the new coordinates of the control points. Let P denote the control polygon and $I(P, L)$ denote the number of times L crosses P. We only need to prove that $I(C, L) \le I(P, L)$.

We set a parameter transformation as $u = \frac{t-a_0}{a_n-t}$, $t \in (a_0, a_n)$, so that $u \in (0, +\infty)$. Then by the Cartesian notation rule

$$I(C, L) = Z_{a_0\le t\le a_n}\left[\sum_{i=0}^{n} y_{a_i} T_{a_i}(t)\right] = Z_{a_0\le t\le a_n}\left[\sum_{i=0}^{n} \frac{y_{a_i}\omega_{a_i}c_{a_i}(t-a_0)^{t-a_i}(a_n-t)^{a_n-a_i}}{\sum_{i=0}^{n}\omega_{a_i}c_{a_i}(t-a_0)^{t-a_i}(a_n-t)^{a_n-a_i}}\right]$$

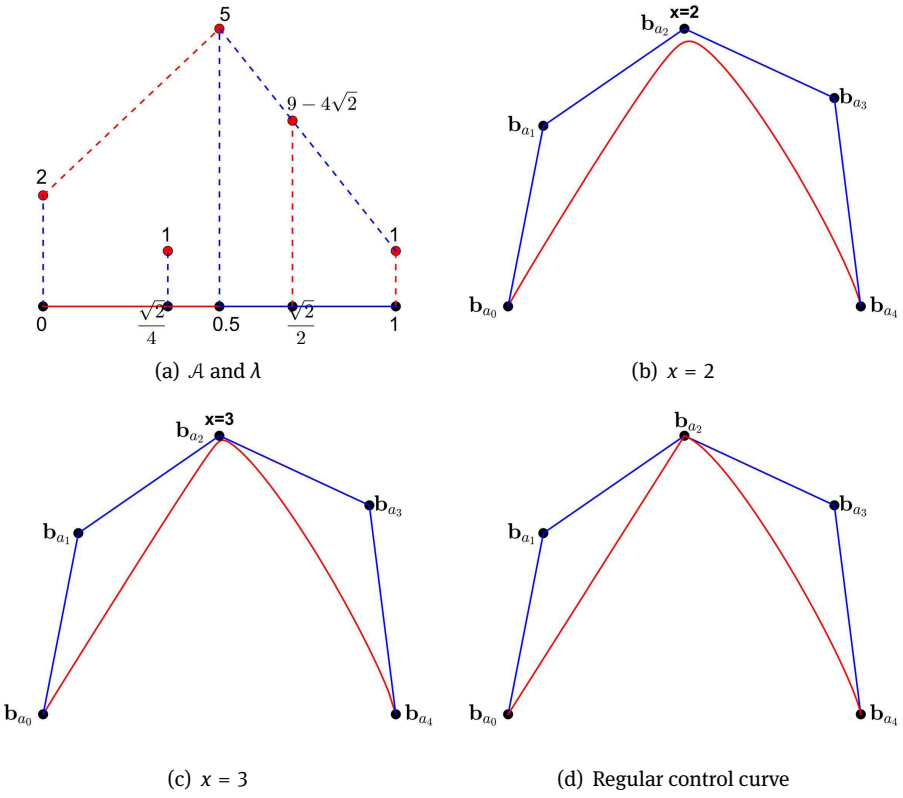

(a) $\mathcal{A}$ and λ (b) $x = 2$

(c) $x = 3$ (d) Regular control curve

Figure 11: Toric degeneration of GT-Bézier curve.

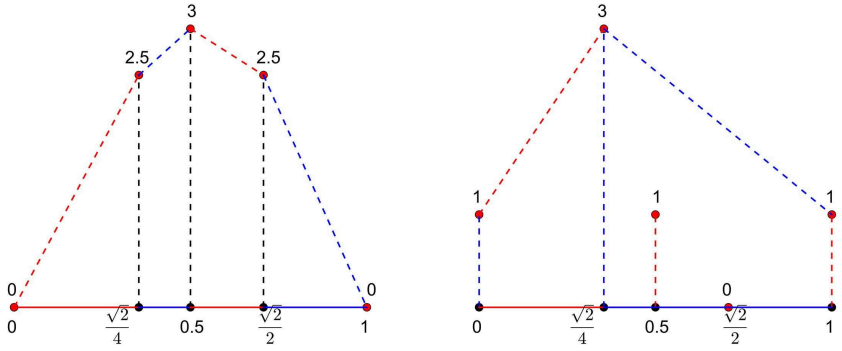

(a) $\mathcal{A}$ and λ' (b) $\mathcal{A}$ and λ''

Figure 12: Regular decompositions of $\mathcal{A}$.

$$
\begin{aligned}
&= Z_{0<u<+\infty}\left[\sum_{i=0}^{n}\frac{y_{a_i}\omega_{a_i}c_{a_i}u^{a_i-a_0}}{\sum_{i=0}^{n}\omega_{a_i}c_{a_i}u^{a_i-a_0}}\right] = Z_{0<u<+\infty}\left[\sum_{i=0}^{n}\frac{y_{a_i}\omega_{a_i}c_{a_i}u^{qd_i}}{\sum_{i=0}^{n}\omega_{a_i}c_{a_i}u^{qd_i}}\right]\\
&= Z_{0<u<+\infty}\left[\sum_{i=0}^{n}\frac{y_{a_i}\omega_{a_i}c_{a_i}u^{qd_i}}{\sum_{i=0}^{n}\omega_{a_i}c_{a_i}u^{qd_i}}\right] = Z_{0<u<+\infty}\left[\sum_{i=0}^{n}y_{a_i}u^{qd_i}\right]\\
&\le V[y_{a_0}, y_{a_1}, \cdots, y_{a_n}] = I(P, L),
\end{aligned}
$$

and this leads to end the proof. □

From Theorem 6, we have the following property.

(i) Convexity-preserving property. Suppose $d_i = a_i - a_0 \in \mathbb{Q}$ $(i = 1, \cdots, n)$, then the planar GT-Bézier curve is convex if its control polygon is convex.

4 Generalized toric-Bézier surfaces

Definition 4. *Let $\mathcal{A} = \{\mathbf{a}_0, \mathbf{a}_1, \cdots, \mathbf{a}_n\} \subset \mathbb{R}^2$ be a finite set of real points. Given positive weights $\omega = \{\omega_{\mathbf{a}_i} \mid \mathbf{a}_i \in \mathcal{A}\}$ and control points $\mathcal{B} = \{\mathbf{b}_{\mathbf{a}_i} \mid \mathbf{a}_i \in \mathcal{A}\}$, the generalized toric-Bézier surface (GT-Bézier surface for short) is defined as*

$$\mathbf{P}_{\mathcal{A},\omega,\mathcal{B}}(u,v) = \sum_{i=0}^{n} \mathbf{b}_{\mathbf{a}_i} T_{\mathbf{a}_i}(u,v) = \sum_{i=0}^{n} \mathbf{b}_{\mathbf{a}_i} \frac{\omega_{\mathbf{a}_i}\beta_{\mathbf{a}_i}(u,v)}{\sum_{i=0}^{n}\omega_{\mathbf{a}_i}\beta_{\mathbf{a}_i}(u,v)}, \quad (u,v) \in \Delta_{\mathcal{A}}. \tag{14}$$

Example 7. *Let $\mathcal{A} = \{(0,2), (1,2), (0,1), (1,1), (2,1), (0,0), (1,0), (2,0)\}$ be the integer points in the pentagon as shown in Figure 1(a). Set control points $\mathcal{B} = \{(0,2,0), (1,2,4), (0, \frac{6}{5}, 2), (\frac{8}{7}, \frac{8}{7}, 5), (2,1,2), (0,0,0), (\frac{6}{5}, 0, 2), (2,0,0)\}$ and weights $\omega = \{2,2,5,7,2,3,5,2\}$. Suppose $c_{\mathbf{a}_i} = 1$ $(i = 0, \cdots, 7)$, then we can define a toric surface as shown in Figure 13(a). This toric surface does not have linear precision, but we can tune it to achieve linear precision. We set $\widetilde{\mathcal{A}} = \{(0,2), (1,2), (0, \frac{6}{5}), (\frac{8}{7}, \frac{8}{7}), (2,1), (0,0), (\frac{6}{5}, 0), (2,0)\}$ by moving the non-extreme points of $\mathcal{A}$ within the pentagon (Figure 1(b)). The GT-Bézier surface constructed by $\widetilde{\mathcal{A}}$, ω and $\mathcal{B}$ has linear precision, as shown in Figure 13(b). The theoretical proof can be found in [24].*

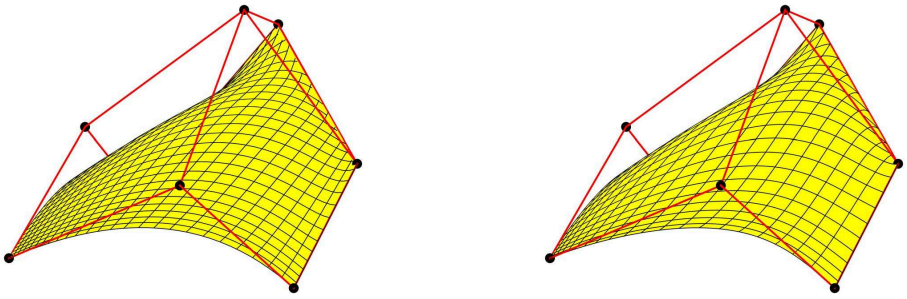

(a) Toric surface (b) GT-Bézier Surface

Figure 13: Toric Surface and GT-Bézier Surface.

From the properties of the GT-Bernstein basis functions, we have the following properties of the GT-Bézier surface.

(a) Affine invariance and convex hull property. Since the basis functions (7) possess of nonnegativity and partition of unity, the corresponding GT-Bézier surface (14) has affine invariance and convex hull property.

(b) Degeneration property. When $\mathcal{A} = \{\mathbf{a}_0, \mathbf{a}_1, \cdots, \mathbf{a}_n\} \subset \mathbb{Z}^2$, the GT-Bézier surface associated of $\mathcal{A}$ degenerates to the toric surface defined in [5] by the property of basis(7). In particular, the rational Bézier triangle defined by $\mathcal{A} = \{(i,j) \in \mathbb{Z}^2 \mid i + j \le k, i \ge 0, j \ge 0\}$, and the rational tensor product Bézier surface defined by $\mathcal{A} = \{(i,j) \in \mathbb{Z}^2 \mid 0 \le i \le m, 0 \le j \ge n\}$ are special cases of the GT-Bézier surface.

(c) Corner points interpolation property. This property follows directly from the property at the corner points property of the basis (7), that is $\mathbf{P}_{\mathcal{A},\omega,\mathcal{B}}(V_i) = \mathbf{b}_{V_i}$, $i = 1, \cdots, r$, where $V_i \in \mathcal{A}$ are the vertices of $\Delta_{\mathcal{A}}$.

(d) Isoparametric curves property. The isoparametric curves $\mathbf{P}_{\mathcal{A},\omega,\mathcal{B}}(u^*, v)$ and $\mathbf{P}_{\mathcal{A},\omega,\mathcal{B}}(u, v^*)$ of a GT-Bézier surface are respectively the GT-Bézier curves.

Theorem 7. *Each boundary of the GT-Bézier surface is a GT-Bézier curve* $\mathbf{P}_{\hat{\phi}_i,\omega|_{\hat{\phi}_i},\mathcal{B}|_{\hat{\phi}_i}}$, *which defined by control points* $\mathbf{b}_{\mathbf{a}_i}$ *and weights* $\omega_{\mathbf{a}_i}$ *by* $\mathbf{a}_i \in \hat{\phi}_i$ *of corresponding edges* $\phi_i \subset \Delta_{\mathcal{A}}$, *where* $i = 1, \cdots, r$.

Proof. Consider the restriction $\mathbf{P}_{\hat{\phi},\omega|_{\hat{\phi}},\mathcal{B}|_{\hat{\phi}}}$ of the GT-Bézier surface at the fixed edge $\phi = \phi_i$ of $\Delta_{\mathcal{A}}$. Denote $V_0 = (u_0, v_0) = V_{i-1}$, $V_1 = (u_1, v_1) = V_i$, and $h_i(u, v) = h(u, v) = \xi u + \eta v + \rho$ is the equation of ϕ for simplicity. Let the angle between the edge ϕ and the u axis be α. Then $\tan\alpha = -\frac{\xi}{\eta}$, and

$$\cos\alpha = \frac{\eta}{\sqrt{\xi^2 + \eta^2}}.$$

Let $\sigma = |V_0V_1| = \sqrt{(u_1 - u_0)^2 + (v_1 - v_0)^2}$. All basis functions $\beta_{\mathbf{a}_i}(u, v)$ with indices $\mathbf{a}_i \in \mathcal{A} \setminus \hat{\phi}$ vanishes if $(u, v) \in \phi$, hence $\mathbf{P}_{\hat{\phi},\omega|_{\hat{\phi}},\mathcal{B}|_{\hat{\phi}}}$ depends only on weights and control points indexed by $\mathbf{a}_i \in \hat{\phi}$. If $\mathbf{a}_j = (u_j, v_j) \in \hat{\phi}$, then $h(\mathbf{a}_j) = \xi u_j + \eta v_j + \rho = 0$, $v_j = -\frac{\rho + \xi u_j}{\eta}$. Let $l_j = |\mathbf{a}_jV_0| = \sqrt{(u_j - u_0)^2 + (v_j - v_0)^2}$. By geometric relationship, we have

$$u_j = u_0 + l_j\cos\alpha.$$

For the edge equation $h_k(u, v) = 0$ for the edge ϕ_k of $\Delta_{\mathcal{A}}$, we evaluate $h_k(u, v)$ at point $\mathbf{a}_j$,

$$\begin{aligned} h_k(\mathbf{a}_j) &= \xi_k u_j + \eta_k v_j + \rho_k \\ &= \frac{\eta\xi_k - \xi\eta_k}{\eta} u_j + \rho_k - \frac{\eta_k}{\eta}\rho \\ &= \rho_k - \frac{\eta_k}{\eta}\rho + \frac{\eta\xi_k - \xi\eta_k}{\eta} u_0 + \frac{(\eta\xi_k - \xi\eta_k)\cos\alpha}{\eta} l_j. \end{aligned}$$

Thus the basis defined on the edge ϕ can be expressed as

$$\beta_{\mathbf{a}_i}(u, v) = c_{\mathbf{a}_i} \prod_{k=1}^{r} h_k(u, v)^{(\rho_k - \frac{\eta_k}{\eta}\rho + \frac{\eta\xi_k - \xi\eta_k}{\eta} u_0)} (h_1(u, v)^{\frac{(\eta\xi_1 - \xi\eta_1)\cos\alpha}{\eta}} \cdots h_r(u, v)^{\frac{(\eta\xi_r - \xi\eta_r)\cos\alpha}{\eta}})^{l_j}.$$

Here the first r factors $h_k(u, v)^{(\rho_k - \frac{\eta_k}{\eta}\rho + \frac{\eta\xi_k - \xi\eta_k}{\eta} u_0)}$ do not depend on j and can be canceled in the definition of GT-Bézier surface.

When $(u, v) \in \phi$, then $h(u, v) = 0$, $v = -\frac{\rho + \xi u}{\eta}$. So when $(u, v) \in \phi$, $h_k(u, v)$ is univariate function of u, written $h_k(u)$. If we set new variables

$$s = h_1(u)^{\frac{(\eta\xi_1 - \xi\eta_1)\cos\alpha}{\eta}} \cdots h_r(u)^{\frac{(\eta\xi_r - \xi\eta_r)\cos\alpha}{\eta}}, \quad t = \frac{\sigma s}{1 + s},$$

we obtain

$$\mathbf{P}_{\hat{\phi},\omega|_{\hat{\phi}},\mathcal{B}|_{\hat{\phi}}}(u) = \frac{\sum_{\mathbf{a}_j \in \hat{\phi}} \omega_{\mathbf{a}_j}\mathbf{b}_{\mathbf{a}_j} c_{\mathbf{a}_j} s^{l_j}}{\sum_{\mathbf{a}_j \in \hat{\phi}} \omega_{\mathbf{a}_j} c_{\mathbf{a}_j} s^{l_j}} = \frac{\sum_{\mathbf{a}_j \in \hat{\phi}} \omega_{\mathbf{a}_j}\mathbf{b}_{\mathbf{a}_j} c_{\mathbf{a}_j} t^{l_j}(\sigma - t)^{\sigma - l_j}}{\sum_{\mathbf{a}_j \in \hat{\phi}} \omega_{\mathbf{a}_j} c_{\mathbf{a}_j} t^{l_j}(\sigma - t)^{\sigma - l_j}}.$$

We choose a natural parameter τ on the edge, $u = u_0 + \tau\sigma\cos\alpha (0 < \tau < 1)$, to prove that this reparametrization is 1-1, and calculate derivatives

$$\begin{aligned} \frac{\mathrm{d}s}{\mathrm{d}\tau} &= \frac{\mathrm{d}}{\mathrm{d}\tau}(h_1(u)^{\frac{(\eta\xi_1 - \xi\eta_1)\cos\alpha}{\eta}}) \cdots h_r(u)^{\frac{(\eta\xi_r - \xi\eta_r)\cos\alpha}{\eta}} + \ldots + h_1(u)^{\frac{(\eta\xi_1 - \xi\eta_1)\cos\alpha}{\eta}} \cdots \frac{\mathrm{d}}{\mathrm{d}\tau}(h_r(u)^{\frac{(\eta\xi_r - \xi\eta_r)\cos\alpha}{\eta}}) \\ &= \sigma \prod_{k=1}^{r} h_k(u)^{\frac{(\eta\xi_k - \xi\eta_k)\cos\alpha}{\eta}} \sum_{j=1}^{r} \frac{(\frac{\eta\xi_j - \xi\eta_j}{\eta}\cos\alpha)^2}{h_j(u)} > 0, \quad 0 < \tau < 1, \end{aligned}$$

and

$$\frac{\mathrm{d}t}{\mathrm{d}\tau}=\frac{\mathrm{d}}{\mathrm{d}\tau}\left(\frac{\sigma s}{1+s}\right)=\frac{\sigma}{(1+s)^2}\frac{\mathrm{d}s}{\mathrm{d}\tau}>0.$$

Hence the reparametrization $\tau \longmapsto t$ is monotonic. Also it is easy to check that it preserves endpoints. Therefore it is 1-1 and ends the proof. □

(e) Multiple knot property. When a knot of $\mathcal{A}$ tends to its adjacent knot, the following theorem describes the limit property of the GT-Bézier surface, and demonstrates the construction of GT-Bézier surface by $\mathcal{A}$ with multiple knots.

Theorem 8. *Suppose* $c_{\mathbf{a}_i}=1(i=0,\cdots,n)$. *When the knot* $\mathbf{a}_k$ $(0\le k<n)$ *approaches to* $\mathbf{a}_q$ $(0\le q<n,$ *and* $q\ne k)$ *along line* $\mathbf{a}_k\mathbf{a}_q$ *with the convex hull* $\Delta_{\mathcal{A}}$ *unchanging, the limit of GT-Bézier surface* $\mathbf{P}_{\mathcal{A},\omega,\mathcal{B}}(u,v)$ *defined in (14) is exactly the GT-Bézier surface* $\widetilde{\mathbf{P}}_{\widetilde{\mathcal{A}},\widetilde{\omega},\widetilde{\mathcal{B}}}(u,v)$, *defined as*

$$\lim_{\mathbf{a}_k\to\mathbf{a}_q}\mathbf{P}_{\mathcal{A},\omega,\mathcal{B}}(u,v)=\widetilde{\mathbf{P}}_{\widetilde{\mathcal{A}},\widetilde{\omega},\widetilde{\mathcal{B}}}(u,v)=\frac{\sum_{i\ne k,q}\omega_{\mathbf{a}_i}\mathbf{b}_{\mathbf{a}_i}\beta_{\mathbf{a}_i}(u,v)+\widetilde{\omega}_{\mathbf{a}_q}\widetilde{\mathbf{b}}_{\mathbf{a}_q}\beta_{\mathbf{a}_q}(u,v)}{\sum_{i\ne k,q}\omega_{\mathbf{a}_i}\beta_{\mathbf{a}_i}(u,v)+\widetilde{\omega}_{\mathbf{a}_q}\beta_{\mathbf{a}_q}(u,v)},\tag{15}$$

where

$$\widetilde{\omega}_{\mathbf{a}_q}=\omega_{\mathbf{a}_k}+\omega_{\mathbf{a}_q},\ \widetilde{\mathbf{b}}_{\mathbf{a}_q}=\frac{\omega_{\mathbf{a}_k}}{\omega_{\mathbf{a}_k}+\omega_{\mathbf{a}_q}}\mathbf{b}_{\mathbf{a}_k}+\frac{\omega_{\mathbf{a}_q}}{\omega_{\mathbf{a}_k}+\omega_{\mathbf{a}_q}}\mathbf{b}_{\mathbf{a}_q},\ \ \widetilde{\omega}=\{\omega_{\mathbf{a}_0},\cdots,\omega_{\mathbf{a}_{k-1}},\omega_{\mathbf{a}_{k+1}},\cdots,\widetilde{\omega}_{\mathbf{a}_q},\cdots,\omega_{\mathbf{a}_n}\},$$
$$\widetilde{\mathcal{A}}=\{\mathbf{a}_0,\cdots,\mathbf{a}_{k-1},\mathbf{a}_{k+1},\cdots,\mathbf{a}_n\},\ \widetilde{\mathcal{B}}=\{\mathbf{b}_{\mathbf{a}_0},\cdots,\mathbf{b}_{\mathbf{a}_{k-1}},\mathbf{b}_{\mathbf{a}_{k+1}},\cdots,\widetilde{\mathbf{b}}_{\mathbf{a}_q},\cdots,\mathbf{b}_{\mathbf{a}_n}\}.\tag{16}$$

Proof. When $\mathbf{a}_k$ tends to $\mathbf{a}_q$, we have

$$\begin{aligned}\lim_{\mathbf{a}_k\to\mathbf{a}_q}\beta_{\mathbf{a}_k}(u,v)&=\lim_{\mathbf{a}_k\to\mathbf{a}_q}h_1(u,v)^{h_1(\mathbf{a}_k)}\cdots h_r(u,v)^{h_r(\mathbf{a}_k)}\\&=h_1(u,v)^{h_1(\mathbf{a}_q)}\cdots h_r(u,v)^{h_r(\mathbf{a}_q)}\\&=\beta_{\mathbf{a}_q}(u,v).\end{aligned}$$

Thus,

$$\begin{aligned}\lim_{\mathbf{a}_k\to\mathbf{a}_q}\sum_{i=0}^{n}\mathbf{b}_{\mathbf{a}_i}T_{\mathbf{a}_i}(u,v)&=\widetilde{\mathbf{P}}_{\widetilde{\mathcal{A}},\widetilde{\omega},\widetilde{\mathcal{B}}}(u,v)\\&=\lim_{\mathbf{a}_k\to\mathbf{a}_q}\sum_{i=0}^{n}\frac{\mathbf{b}_{\mathbf{a}_i}\omega_{\mathbf{a}_i}\beta_{\mathbf{a}_i}(u,v)}{\sum_{i=0}^{n}\omega_{\mathbf{a}_i}\beta_{\mathbf{a}_i}(u,v)}\\&=\frac{\sum_{i\ne k,q}\omega_{\mathbf{a}_i}\mathbf{b}_{\mathbf{a}_i}\beta_{\mathbf{a}_i}(u,v)+\omega_{\mathbf{a}_k}\mathbf{b}_{\mathbf{a}_k}\beta_{\mathbf{a}_q}(u,v)+\omega_{\mathbf{a}_q}\mathbf{b}_{\mathbf{a}_q}\beta_{\mathbf{a}_q}(u,v)}{\sum_{i\ne k,q}\omega_{\mathbf{a}_i}\beta_{\mathbf{a}_i}(u,v)+\omega_{\mathbf{a}_k}\beta_{\mathbf{a}_q}(u,v)+\omega_{\mathbf{a}_q}\beta_{\mathbf{a}_q}(u,v)}\\&=\frac{\sum_{i\ne k,q}\omega_{\mathbf{a}_i}\mathbf{b}_{\mathbf{a}_i}\beta_{\mathbf{a}_i}(u,v)+(\omega_{\mathbf{a}_k}\mathbf{b}_{\mathbf{a}_k}+\omega_{\mathbf{a}_q}b_{\mathbf{a}_q})\beta_{\mathbf{a}_q}(u,v)}{\sum_{i\ne k,q}\omega_{\mathbf{a}_i}\beta_{\mathbf{a}_i}(u,v)+(\omega_{\mathbf{a}_k}+\omega_{\mathbf{a}_q})\beta_{\mathbf{a}_q}(u,v)}.\end{aligned}$$

Let $\widetilde{\omega}_{\mathbf{a}_q}=\omega_{\mathbf{a}_k}+\omega_{\mathbf{a}_q}$, $\widetilde{\mathbf{b}}_{\mathbf{a}_q}=\frac{\omega_{\mathbf{a}_k}}{\omega_{\mathbf{a}_k}+\omega_{\mathbf{a}_q}}\mathbf{b}_{\mathbf{a}_k}+\frac{\omega_{\mathbf{a}_q}}{\omega_{\mathbf{a}_k}+\omega_{\mathbf{a}_q}}\mathbf{b}_{\mathbf{a}_q}$, we can obtain

$$\lim_{\mathbf{a}_k\to\mathbf{a}_q}\mathbf{P}_{\mathcal{A},\omega,\mathcal{B}}(u,v)=\widetilde{\mathbf{P}}_{\widetilde{\mathcal{A}},\widetilde{\omega},\widetilde{\mathcal{B}}}(u,v)=\frac{\sum_{i\ne k,q}\omega_{\mathbf{a}_i}\mathbf{b}_{\mathbf{a}_i}\beta_{\mathbf{a}_i}(u,v)+\widetilde{\omega}_{\mathbf{a}_q}\widetilde{\mathbf{b}}_{\mathbf{a}_q}\beta_{\mathbf{a}_q}(u,v)}{\sum_{i\ne k,q}\omega_{\mathbf{a}_i}\beta_{\mathbf{a}_i}(u,v)+\widetilde{\omega}_{\mathbf{a}_q}\beta_{\mathbf{a}_q}(u,v)},$$

where $\widetilde{\mathcal{A}}=\{\mathbf{a}_0,\cdots,\mathbf{a}_{k-1},\mathbf{a}_{k+1},\cdots,\mathbf{a}_n\}$, $\widetilde{\mathcal{B}}=\{\mathbf{b}_{\mathbf{a}_0},\cdots,\mathbf{b}_{\mathbf{a}_{k-1}},\mathbf{b}_{\mathbf{a}_{k+1}},\cdots,\widetilde{\mathbf{b}}_{\mathbf{a}_q},\cdots,\mathbf{b}_{\mathbf{a}_n}\}$ and $\widetilde{\omega}=\{\omega_{\mathbf{a}_0},\cdots,\omega_{\mathbf{a}_{k-1}},\omega_{\mathbf{a}_{k+1}},\cdots,\widetilde{\omega}_{\mathbf{a}_q},\cdots,\omega_{\mathbf{a}_n}\}$. □

Example 8. *Consider the GT-Bézier surface defined in Example 7. Let* $\mathcal{A}=\{(0,2),(1,2),(0,\frac{6}{5}),(\frac{8}{7},\frac{8}{7}),(2,1),(0,0),(\frac{6}{5},0),(2,0)\}$, *control points* $\mathcal{B}=\{(0,2,0),(1,2,4),(0,\frac{6}{5},2),(\frac{8}{7},\frac{8}{7},5),(2,1,2),(0,0,0),$

$(\frac{6}{5}, 0, 2), (2, 0, 0)\}$, *weights* $\omega = \{2, 2, 5, 7, 2, 3, 5, 2\}$ *and* $c_{\mathbf{a}_i} = 1\,(i = 0, \cdots, 7)$. *If* $\mathbf{a}_3 = (\frac{8}{7}, \frac{8}{7})$ *approaches* $\mathbf{a}_1 = (1, 2)$, *then the changes of the GT-Bézier surface are shown in Figure 14.*

Since the shape of the convex hull $\Delta_{\mathcal{A}}$ *and control points* $\mathcal{B}$ *are unchanging during the process of* $\mathbf{a}_3$ *tending to* $\mathbf{a}_1$, *the original curved surface is stretched like an elastic film by the boundary property of the GT-Bézier surface. Until* $\mathbf{a}_3 = \mathbf{a}_1$, *the resulting surface is defined by* $\widetilde{\mathcal{A}} = \{(0, 2), (1, 2), (0, \frac{6}{5}), (2, 1), (0, 0), (\frac{6}{5}, 0), (2, 0)\}$, *control points* $\widetilde{\mathcal{B}} = \{(0, 2, 0), (\frac{10}{9}, \frac{12}{9}, \frac{43}{9}), (0, \frac{6}{5}, 2), (2, 1, 2), (0, 0, 0), (\frac{6}{5}, 0, 2), (2, 0, 0)\}$, *weights* $\widetilde{\omega} = \{2, 9, 5, 2, 3, 5, 2\}$.

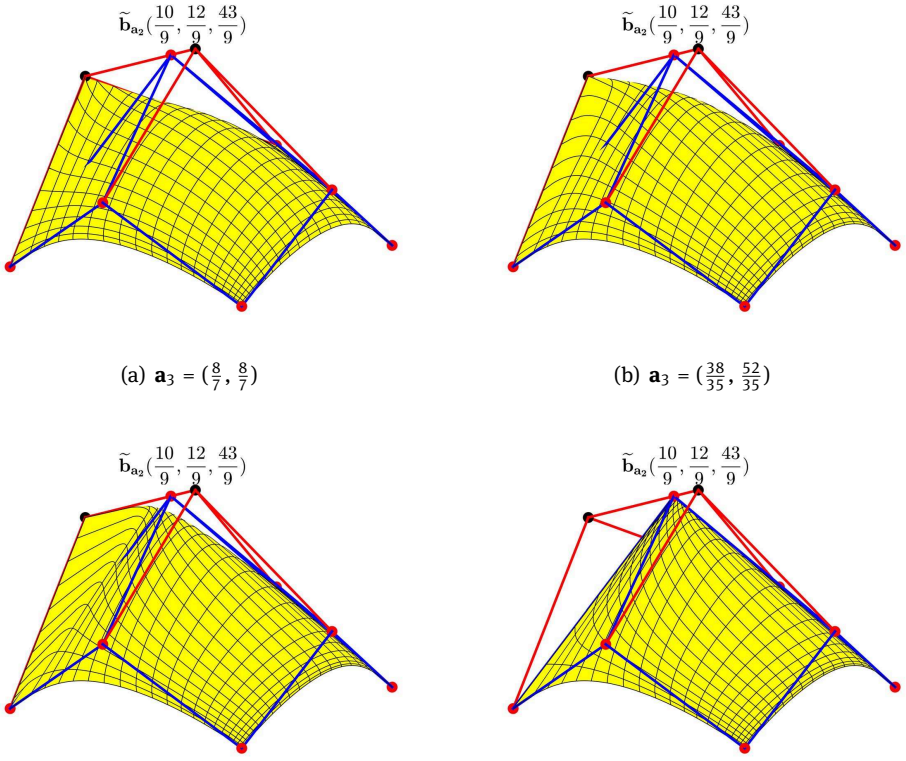

(a) $\mathbf{a}_3 = (\frac{8}{7}, \frac{8}{7})$ (b) $\mathbf{a}_3 = (\frac{38}{35}, \frac{52}{35})$

(c) $\mathbf{a}_3 = (\frac{36}{35}, \frac{64}{35})$ (d) Limit surface

Figure 14: Limit of GT-Bézier surface with $\mathbf{a}_3 \to \mathbf{a}_1$.

Theorem 8 shows that the limit surface of the GT-Bézier surface when single knot approaches to another with the convex hull $\Delta_{\mathcal{A}}$ unchanging. For the limit of multiple knots with the convex hull $\Delta_{\mathcal{A}}$ unchanging, we only need to treat it by Theorem 8 repeatedly.

(f) Toric degeneration property. Similarly, let $\lambda : \mathcal{A} \to \mathbb{R}$ be a lifting function to lift the points $\mathbf{a}_i$ of $\mathcal{A}$ to $(\mathbf{a}_i, \lambda(\mathbf{a}_i)) \in \mathbb{R}^3$. We denote $P_\lambda = conv\{(\mathbf{a}_i, \lambda(\mathbf{a}_i)) \mid \mathbf{a}_i \in \mathcal{A}\}$ the convex hull of the lifted points. Each face of the convex hull P_λ has a normal vector pointing to the outer side. We call it the upper face of P_λ if the last coordinate of the normal vector is positive. If we project these upper faces back vertically into $\mathbb{R}^2$, they can cover $\Delta_{\mathcal{A}}$ and form a regular subdivision Γ_λ of $\Delta_{\mathcal{A}}$ induced by λ (see [6]).

We group together the points of $\mathcal{A}$ that are in the same subset of the Γ_λ and on the same upper face of the P_λ. Then we get a decomposition of $\mathcal{A}$, which is called regular decomposition $\mathcal{S}_\lambda$ of $\mathcal{A}$ induced by λ. For each subset $\mathcal{F}$ of $\mathcal{S}_\lambda$, we can use the weights $\omega|_{\mathcal{F}} = \{\omega_{\mathbf{a}_i} \mid \mathbf{a}_i \in \mathcal{F}\}$ and the control points $\mathcal{B}|_{\mathcal{F}} = \{\mathbf{b}_{\mathbf{a}_i} \mid \mathbf{a}_i \in \mathcal{F}\}$ to define a new GT-Bézier surface $\mathbf{P}_{\mathcal{F}, \omega|_{\mathcal{F}}, \mathcal{B}|_{\mathcal{F}}}$ on $\Delta_{\mathcal{F}} = conv\{\mathbf{a}_i \in \mathcal{F}\}$ by Definition 4.

The union of these patches

$$\mathbf{P}_{\mathcal{A},\omega,\mathcal{B}}(\mathcal{S}_\lambda) = \bigcup_{\mathcal{F}\in\mathcal{S}_\lambda} \mathbf{P}_{\mathcal{F},\omega|_{\mathcal{F}},\mathcal{B}|_{\mathcal{F}}}$$

is called the regular control surface of $\mathbf{P}_{\mathcal{A},\omega,\mathcal{B}}$ induced by regular decomposition $\mathcal{S}_\lambda$.

We can use lifting function λ to get a set of weights with a parameter x, $\omega_\lambda(x) := \{x^{\lambda(\mathbf{a}_i)}\omega_{\mathbf{a}_i} \mid \mathbf{a}_i \in \mathcal{A}\}$. These weights are used to define the map

$$\mathbf{P}_{\mathcal{A},\omega_\lambda(x),\mathcal{B}}(u,v)=\frac{\sum_{i=0}^{n} x^{\lambda(\mathbf{a}_i)}\omega_{\mathbf{a}_i}\mathbf{b}_{\mathbf{a}_i}\beta_{\mathbf{a}_i}(u,v)}{\sum_{i=0}^{n} x^{\lambda(\mathbf{a}_i)}\omega_{\mathbf{a}_i}\beta_{\mathbf{a}_i}(u,v)}, \quad (u,v)\in\Delta_{\mathcal{A}}. \tag{17}$$

The image of $\Delta_{\mathcal{A}}$ under this map is a GT-Bézier surface with a parameter x, denoted as $\mathbf{P}_{\mathcal{A},\omega_\lambda(x),\mathcal{B}}$. We have the following result.

Theorem 9. *The limit of the GT-Bézier surface $\mathbf{P}_{\mathcal{A},\omega_\lambda(x),\mathcal{B}}$ as $x\to\infty$ is the regular control surface induced by the regular decomposition $\mathcal{S}_\lambda$, that is*

$$\lim_{x\to\infty} \mathbf{P}_{\mathcal{A},\omega_\lambda(x),\mathcal{B}} = \mathbf{P}_{\mathcal{A},\omega,\mathcal{B}}(\mathcal{S}_\lambda).$$

Proof. The proof of the theorem is similar to Theorem 5 and will be omitted here. □

Theorem 9 describes the conclusion that the limit surface of the GT-Bézier surface is its regular control surface, and explains the geometric meaning of the limit surface of the GT-Bézier surface when all the weights tend to infinity. And this property is called toric degeneration of GT-Bézier surfaces.

Example 9.
Given point set $\widetilde{\mathcal{A}}$ is shown in Figure 1(b), and the lifted values of $\widetilde{\mathcal{A}}$ by λ are shown in Figure 15(a). The upper hull and the subdivision of $\Delta_{\widetilde{\mathcal{A}}}$ by λ are shown in Figure 15(b), and the regular decomposition $\mathcal{S}_\lambda$ is shown in Figure 15(c). Let control points $\mathcal{B} = \{(0,2,0),(1,2,4),(0,\frac{6}{5},2),(\frac{8}{7},\frac{8}{7},18),(2,1,2),(0,0,0),(\frac{6}{5},0,2),(2,0,0)\}$ and weights $\omega = \{2,2,5,7,2,3,5,2\}$ corresponding to $\widetilde{\mathcal{A}}$. The toric degeneration process of this GT-Bézier surface is shown in Figure 16. This figure also shows the GT-Bézier surfaces for the parameters $x = 5$, $x = 100$ and $x = 600$ respectively. As the parameter x becomes larger, the GT-Bézier surface approaches its regular control surface in Figure 16(d) (consists of surface patches defined by three triangles and two quadrilaterals).

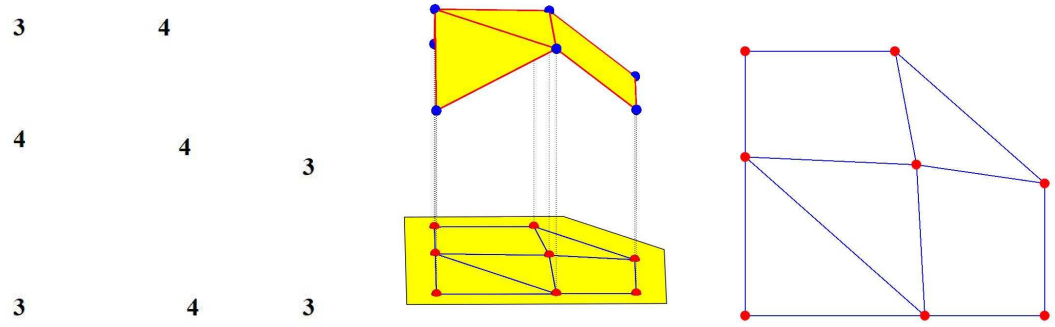

(a) λ (b) Upper hull and projection (c) Decomposition

Figure 15: Regular decomposition.

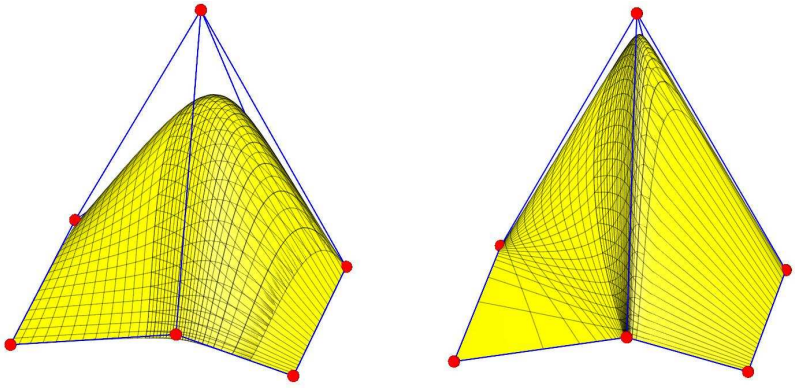

(a) $x = 5$ (b) $x = 100$

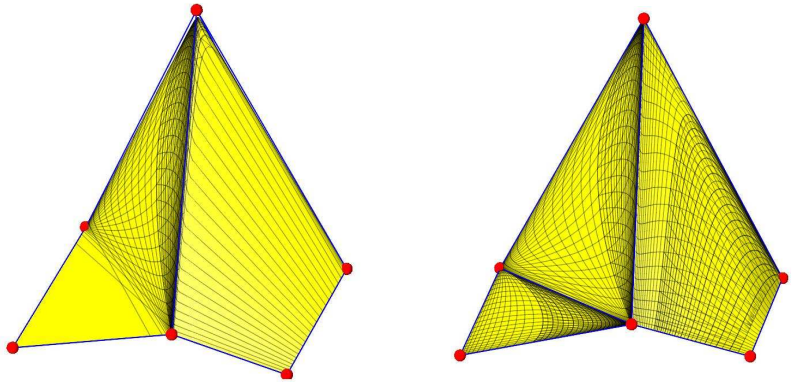

(c) $x = 600$ (d) Regular control surface

Figure 16: Toric degeneration of GT-Bézier surface.

5 Conclusions and future work

In this paper, we present novel generalized toric-Bézier (GT-Bézier) curves and surfaces and discuss their properties. Firstly, we define a new kind of blending functions associated with a real points set, called generalized toric-Bernstein (GT-Bernstein) basis functions. The degree of GT-Bernstein basis functions is an arbitrary real number. Secondly, the corresponding generalized toric-Bézier (GT-Bézier) curves and surfaces are constructed, which are the projections of the (irrational) toric varieties in fact and the generalizations of the classical rational Bézier curves/surfaces and toric surface patches. Furthermore, we also study the properties of the presented curves and surfaces, including the limiting properties of weights and knots. We indicate that the GT-Bézier curve and surface we presented partially preserve the properties of rational Bézier curves and surfaces. Finally, some representative examples verify the properties and results.

Our further work will be devoted to elevation algorithm and de Casteljau algorithm of GT-Bézier curves and surfaces. In addition, although the basis defined by real knots limits the application in computation, it provides a wider of shapes for design. In this paper, we present the definition and study the properties of curves and surfaces theoretically only. We will study the applications of GT-Bézier curves and surfaces in future, such as barycentric coordinate construction, shape deformation, computer animation, and surface construction by PIA method.

Acknowledgements: The authors appreciate the valuable comments and suggestions from the anonymous reviewers, which improve the clarity of the paper. This work is partly supported by the National Natural Science Foundation of China (Nos. 11671068, 11801053).

References

[1] G. J. Wang, G. Z. Wang, and J. M. Zheng, *Computer Aided Geometric Design*, Higher Education Press, Bei Jing, 2001.

[2] G. Farin, *Curves and Surfaces for CAGD: A Practical Guide*, Morgan Kaufmann, San Francisco, 2002.

[3] *Bézier surface*, https://en.wikipedia.org/wiki/Bézier_surface.

[4] J. Warren, *Creating multisided rational Bézier surfaces using base points*, ACM Trans. Graph. **11** (1992), no. 2, 127–139, DOI: 10.1145/130826.130828.

[5] R. Krasauskas, *Toric surface patches*, Adv. Comput. Math. **17** (2002), no. 1-2, 89–113, DOI: 10.1023/A:1015289823859.

[6] L. D. García-Puente, F. Sottile, and C. G. Zhu, *Toric degenerations of Bézier patches*, ACM Trans. Graph. **30** (2011), no. 5, 1–10, DOI: 10.1145/2019627.2019629.

[7] J. W. Zhang, *C-curves: An extension of cubic curves*, Comput. Aided Geom. Design. **13** (1996), no. 3, 199–217, DOI: 10.1016/0167-8396(95)00022-4.

[8] J. W. Zhang, *C-Bézier curves and surfaces*, Graphical Models & Image Process. **61** (1999), no. 1, 2–15, DOI: 10.1006/gmip.1999.0490.

[9] Q. Y. Chen and G. J. Wang, *A class of Bézier-like curves*, Comput. Aided Geom. Design. **20** (2003), no. 1, 29–39, DOI: 10.1016/s0167-8396(03)00003-7.

[10] G. J. Wang, Q. Y. Chen, and M. H. Zhou, *NUAT B-spline curves*, Comput. Aided Geom. Design. **21** (2004), no. 2, 193–205, DOI: 10.1016/j.cagd.2003.10.002.

[11] H. Oruç and G. M. Phillips, *q-Bernstein polynomials and Bézier curves*, J. Comput. Appl. Math. **151** (2003), no. 1, 1–12, DOI: 10.1016/S0377-0427(02)00733-1.

[12] G. M. Phillips, *Bernstein polynomials based on the q-integers*, Ann. Numer. Math. **4** (1997), no. 1, 511–518, DOI: 10.1007/0-387-21682-0_7.

[13] L. W. Han, Y. Chu, and Z. Y. Qiu, *Generalized Bézier curves and surfaces based on Lupaş q-analogue of Bernstein operator*, J. Comput. Appl. Math. **261** (2014), no. 4, 352–363, DOI: 10.1016/j.cam.2013.11.016.

[14] Q. B. Cai, G. R. Zhou, and J. J. Li, *Statistical approximation properties of λ-Bernstein operators based on q-integers*, Open Math. **17** (2019), no. 1, 487–498, DOI: 10.1515/math-2019-0039.

[15] G. Hu, J. L. Wu, and X. Q. Qin, *A novel extension of the Bézier mode and its applications to surface modeling*, Adv. Eng. Softw. **125** (2018), 27–54, DOI: 10.1016/j.advengsoft.2018.09.002.

[16] G. Hu and J. L. Wu, *Generalized quartic H-Bézier curves: Construction and application to developable surfaces*, Adv. Eng. Softw. **138** (2019), 102723, DOI: 10.1016/j.advengsoft.2019.102723.

[17] R. Schaback, *Creating surfaces from scattered data using radial basis functions*, in: M. Dæhlen, T. Lyche, and L. L. Schumaker (Eds.), Mathematical Methods for Curves and Surfaces, Vanderbilt University Press, Nashville, TN, **38** (1995), no. 4, 477–496.

[18] R. Goldman and P. Simeonov, *Quantum Bernstein bases and quantum Bézier curves*, J. Comput. Appl. Math. **288** (2015), 284–303, DOI: 10.1016/j.cam.2015.04.027.

[19] G. R. Zhou and Q. B. Cai, *Triangular surface patch based on bivariate Meyer-König-Zeller operator*, Open Math. **17** (2019), no. 1, 282–296, DOI: 10.1515/math-2019-0021.

[20] G. R. Zhou, X. M. Zeng, and F. L. Fan, *Bivariate S-λ bases and S-λ surface patches*, Comput. Aided Geom. Design. **31** (2014), 674–688, DOI: 10.1016/j.cagd.2014.08.004.

[21] P. Salvi and T. Várady, *Multi-sided Bézier surfaces over concave polygonal domains*, Comput Graph. **74** (2018), 56–65, DOI: 10.1016/j.cag.2018.05.006.

[22] T. Várady, P. Salvi, and G. Karikó, *A multi-sided Bézier patch with a simple control structure*, Comput Graph. Forum **35** (2016), no. 2, 307–317, DOI: 10.1111/cgf.12833.

[23] Y. P. Zhu, X. L. Han, and S. J. Liu, *Curve construction based on four αβ-Bernstein-like basis functions*, J. Comput. Appl. Math. **273** (2015), 160–181, DOI: 10.1016/j.cam.2014.06.014.

[24] L. D. García-Puente and F. Sottile, *Linear precision for parametric patches*, Adv. Comput. Math. **33** (2010), no. 2, 191–214, DOI: 10.1007/s10444-009-9126-7.

[25] G. Craciun, L. D. García-Puente, and F. Sottile, *Some geometrical aspects of control points for toric patches*, in: M. Dæhlen, et al., (Eds.), Mathematical Methods for Curves and Surfaces, Springer, Berlin, Heidelberg, LNCS **5862** (2008), 111–135, DOI: 10.1007/978-3-642-11620-9_9.

[26] L. Pachter and B. Sturmfels, *Algebraic Statistics for Computational Biology*, Cambridge University Press, Cambridge, 2005, 1183–1202.

[27] E. Postinghel, F. Sottile, and N. Villamizar, *Degenerations of real irrational toric varieties*, J. Lond. Math. Soc. **92** (2015), no. 2, 223–241, DOI: 10.1112/jlms/jdv024.

[28] A. F. Pir and F. Sottile, *Irrational Toric Varieties*, arXiv:1807.05919.

[29] J. G. Li, Q. Y. Chen, J. Q. Han, Q. L. Huang, and C. G. Zhu, *A new kind of parametric curves by special basis function*, Comput. Sci. **45** (2018), no. 3, 46–50, DOI: 10.11896/j.issn.1002-137X.2018.03.007.

[30] Y. Zhang and C. G. Zhu, *Degenerations of NURBS curves while all of weights approaching infinity*, Jpn. J. Ind. Appl. Math. **35** (2018), no. 2, 787–816, DOI: 10.1007/s13160-018-0301-4.

[31] H. W. Lin, H. J. Bao, and G. J. Wang, *Totally positive bases and progressive iteration approximation*, Comput. Math. Appl. **50** (2005), no. 3, 575–586, DOI: 10.1016/j.camwa.2005.01.023.

[32] Y. Y. Yu, H. Ma, and C. G. Zhu, *Total positivity of a kind of generalized toric-Bernstein basis*, Linear Algebra Appl. **579** (2019), 449–462, DOI: 10.1016/j.laa.2019.06.012.

[33] C. G. Zhu and X. Y. Zhao, *Self-intersections of rational Bézier curves*, Graph. Models **76** (2014), no. 5, 312–320, DOI: 10.1016/j.gmod.2014.04.001.